MODELING AND CONTROL OF HYBRID AC/DC MICRO GRID

A Thesis Submitted in Partial Fulfillment

of the Requirements for the Award of the Degree of

Master of Technology
in
Power Control & Drives

by
Lipsa Priyadarshanee

Department of Electrical Engineering

National Institute of Technology

Rourkela-769008

MODELING AND CONTROL OF HYBRID AC/DC MICROGRID

A Thesis Submitted in Partial Fulfillment

of the Requirements for the Award of the Degree of

Master of Technology

in

Power Control & Drives

by

Lipsa Priyadarshanee

(210EE2108)

Under the supervision

of

Prof. Anup Kumar Panda

Department of Electrical Engineering

National Institute of Technology

Rourkela-769008

Dedicated to my beloved parents & brother

DEPARTMENT OF ELECTRICAL ENGINEERING

NATIONAL INSTITUTE OF TECHNOLOGY, ROURKELA

ODISHA, INDIA

CERTIFICATE

This is to certify that the Thesis Report entitled "MODELING AND CONTROL OF HYBRID AC/DC MICROGRID", submitted by Ms. LIPSA PRIYADARSHANEE bearing roll no. 210EE2108 in partial fulfillment of the requirements for the award of Master of Technology in Electrical Engineering with specialization in "Power Control and Drives" during session 2010-2012 at National Institute of Technology, Rourkela is an authentic work carried out by him under our supervision and guidance.

To the best of our knowledge, the matter embodied in the thesis has not been submitted to any other university/institute for the award of any Degree or Diploma.

Date:

Place: Rourkela

Prof. A. K. Panda

Department of Electrical Engineering

National Institute of Technology

Rourkela – 769008

Email: akpanda@nitrkl.ac.in

ACKNOWLEDGEMENT

With deep regards and profound respect, I avail this opportunity to express my deep sense of gratitude and indebtedness to my supervisor Professor Anup Kumar Panda, Electrical Engineering Department, National Institute of Technology, Rourkela for his inspiring guidance, constructive criticism and valuable suggestion throughout this work. It would have not been possible for me to bring out this thesis without his help and constant encouragement. I am also thankful to all faculty members and research students of Electrical Department, NIT Rourkela. I am especially grateful to Power Electronics Laboratory staff Mr. Rabindra Nayak without him the work would have not progressed.

Most important of all, I would like to express my gratitude to my parents, my brother and best of friends for their constant love, affection, endless encouragement and noble devotion to my education. I am enormously grateful to all my close friends of NIT Rourkela for supporting me in all circumstances and making my stay here memorable. I am truly indebted to all my friends and relatives for their kind support. I am also equally thankful to all those who have contributed, directly or indirectly, to this present work. Last but not the least; I am sure this section would not come to an end without remaining indebted to God Almighty, the Guide of all guides who has dispelled the envelope of my ignorance with his radiance of knowledge. I dedicate this thesis to my family, brother Pintu and best friends Tapu and Subh.

Lipsa Priyadarshanee

ABSTRACT

Renewable energy based distributed generators (DGs) play a dominant role in electricity production, with the increase in the global warming. Distributed generation based on wind, solar energy, biomass, mini-hydro along with use of fuel cells and microturbines will give significant momentum in near future. Advantages like environmental friendliness, expandability and flexibility have made distributed generation, powered by various renewable and nonconventional microsources, an attractive option for configuring modern electrical grids. A microgrid consists of cluster of loads and distributed generators that operate as a single controllable system. As an integrated energy delivery system microgrid can operate in parallel with or isolated from the main power grid. The microgrid concept introduces the reduction of multiple reverse conversions in an individual AC or DC grid and also facilitates connections to variable renewable AC and DC sources and loads to power systems. The interconnection of DGs to the utility/grid through power electronic converters has risen concerned about safe operation and protection of equipment's. To the customer the microgrid can be designed to meet their special requirements; such as, enhancement of local reliability, reduction of feeder losses, local voltages support, increased efficiency through use of waste heat, correction of voltage sag or uninterruptible power supply. In the present work the performance of hybrid AC/DC microgrid system is analyzed in the grid tied mode. Here photovoltaic system, wind turbine generator and battery are used for the development of microgrid. Also control mechanisms are implemented for the converters to properly co-ordinate the AC sub-grid to DC sub-grid. The results are obtained from the MATLAB/ SIMULINK environment.

TABLE OF CONTENTS

LIST OF FIGURES

LIST OF TABLES

ACRONYMS

I_{pv}	Terminal voltage of PV module
V_{pv}	Output current of PV module
I_{PH}	Light generated current or photocurrent
I_S	Module reverse saturated current
I_{SC}	Cell's short-circuit current
I_{RS}	Cell's reverse saturation current at reference temperature
V_{OC}	Open circuit voltage
q	Electron charge
k	Boltzmann’s constant
A	Ideal factor
K_I	cell’s short-circuit current temperature coefficient
E_G	Energy of the band gap of the silicon
T_C	Cell's working Temperature
T_{Ref}	Cell's reference Temperature
λ	Solar irradiation
R_S	Series resistance of PV cell
R_{SH}	Parallel resistance of PV cell
N_P	Number of cells in parallel
N_s	Number of cells in series
P_{max}	Maximum power
V_{max}	Terminal voltage of PV cell at MPP

I_{max}	Output current of PV cell at MPP
γ	Cell fill factor of PV cell
V_b	Terminal voltage of battery
V_0	Open circuit voltage of battery
R_b	Internal resistance of battery
i_b	Battery charging current
K	Polarization voltage
Q	Battery capacity
A	Exponential voltage
B	Exponential capacity
SOC	State of charge of battery
P_{air}	Power contained in wind
ρ	The air density
A	The swept area
V_∞	The wind velocity without rotor interference
C_p	Power coefficient
λ	Tip speed ratio
ω	Rotational speed of rotor
R	The radius of the swept area
v_{ds}^s	d^s-axis stator voltage
v_{qs}^s	q^s-axis stator voltage
v_{dr}^s	d^r-axis rotor voltage

v_{qr}^{s}	q^{r}-axis rotor voltage
v_{ds}	d-axis stator voltage
v_{qs}	q-axis stator voltage
v_{dr}	d-axis rotor voltage
v_{qr}	q-axis rotor voltage
i_{ds}^{s}	d^{s}-axis stator current
i_{qs}^{s}	q^{s}-axis stator current
i_{dr}^{s}	d^{r}-axis rotor current
i_{qr}^{s}	q^{r}-axis rotor current
i_{ds}	d-axis stator current
i_{qs}	q-axis stator current
i_{dr}	d-axis rotor current
i_{qr}	q-axis rotor current
λ_{ds}^{s}	d^{s}-axis stator flux linkage
λ_{qs}^{s}	q^{s}-axis stator flux linkage
λ_{dr}^{s}	d^{r}-axis rotor flux linkage
λ_{qr}^{s}	q^{r}-axis rotor flux linkage
λ_{ds}	d-axis stator flux linkage
λ_{qs}	q-axis stator flux linkage
λ_{dr}	d-axis rotor flux linkage
λ_{qr}	q-axis rotor flux linkage
θ^{e}	Angle of synchronously rotating frame

θ	Angle of stationary reference frame
R_s	Stator resistance
R_r	Rotor resistance with respect to stator
ω_e	Synchronous speed
ω_r	Rotor electrical speed
ω_m	Rotor mechanical speed
ω_b	Angular frequency
f	Supply frequency
L_{1s}	Stator leakage inductance
L_{1r}	Rotor leakage inductance
L_s	Stator inductance
L_r	Rotor inductance
L_m	Magnetizing inductance
P	Number of poles
T_e	Electromagnetic torque
T_L	Load torque
J	Rotor inertia
B	Damping constant
P_s	Active power in the grid
Q_s	Reactive power in the grid
v_d	d-axis grid voltage
v_q	q-axis grid voltage

i_d	d-axis grid current
i_q	q-axis grid current
R	Line resistance
L	Line inductance
C	DC-link capacitance
v_{dc}	DC-link voltage
m_1	Modulation index of supply side converter
m_2	Modulation index of machine side converter
P_{cur}	Rotor copper loss
P_{cus}	Stator copper loss
X_{1s}	Stator leakage reactance
X_{1r}	Rotor leakage reactance
X_s	Stator reactance
X_r	Rotor reactance
X_m	Magnetizing reactance
C_{pv}	Capacitor across the solar panel
L_1	Inductor for the boost converter
C_d	Capacitor across the DC-link
L_2	Filtering inductor for the inverter
R_2	Equivalent resistance of the inverter
C_2	Filtering capacitor for the inverter
L_3	Inductor for the battery converter

R_3	Resistance of L_3
f	Frequency of the AC grid
f_s	Switching frequency for the power converter
V_d	Rated DC bus voltage

CHAPTER 1

INTRODUCTION TO MICROGRID

1.1. Introduction

1.1.1. General information regarding microgrid

As electric distribution technology steps into the next century, many trends are becoming noticeable that will change the requirements of energy delivery. These modifications are being driven from both the demand side where higher energy availability and efficiency are desired and from the supply side where the integration of distributed generation and peak-shaving technologies must be accommodated [1].

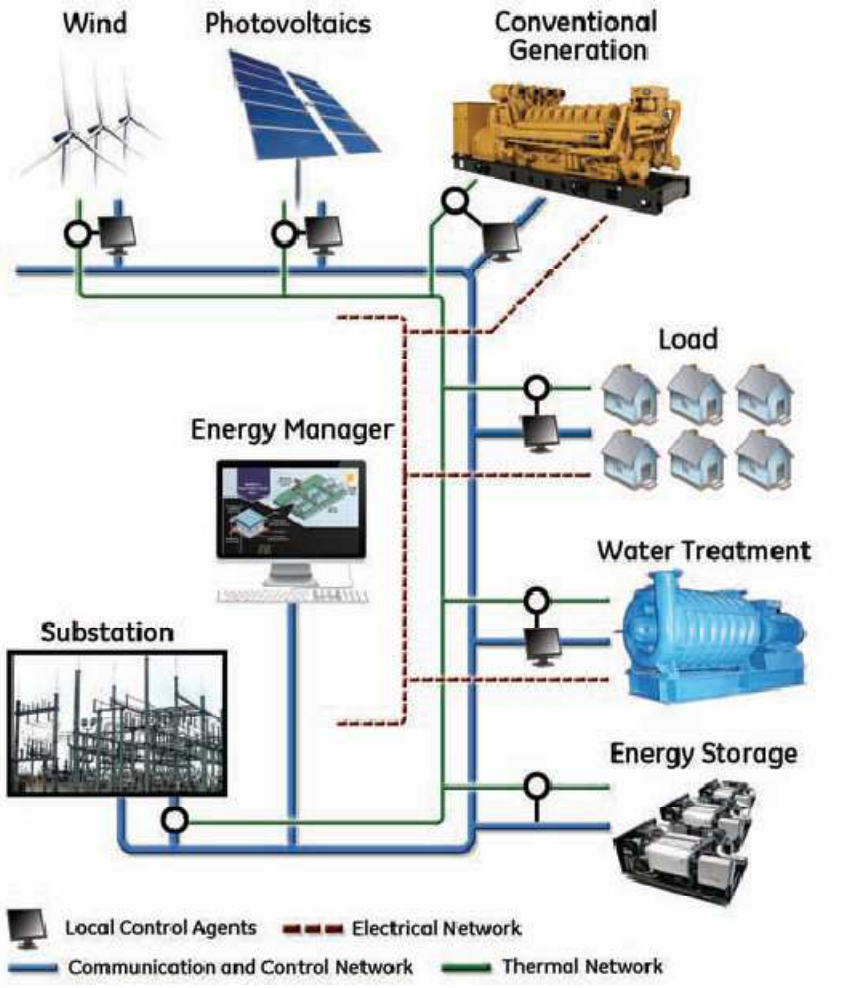

Fig 1.1. Microgrid power system

Power systems currently undergo considerable change in operating requirements mainly as a result of deregulation and due to an increasing amount of distributed energy resources (DER). In many cases DERs include different technologies that allow generation in small scale (microsources) and some of them take advantage of renewable energy resources (RES) such as solar, wind or hydro energy. Having microsources close to the load has the advantage of reducing transmission losses as well as preventing network congestions. Moreover, the possibility of having a power supply interruption of end-customers connected to a low voltage (LV) distribution grid (in Europe 230 V and in the USA 110 V) is diminished since adjacent microsources, controllable loads and energy storage systems can operate in the islanded mode in case of severe system disturbances. This is identified nowadays as a microgrid. Figure 1.1 depicts a typical microgrid. The distinctive microgrid has the similar size as a low voltage distribution feeder and will rare exceed a capacity of 1 MVA and a geographic span of 1 km. Generally more than 90% of low voltage domestic customers are supplied by underground cable when the rest is supplied by overhead lines. The microgrid often psupplies both electricity and heat to the customers by means of combined heat and power plants (CHP), gas turbines, fuel cells, photovoltaic (PV) systems, wind turbines, etc. The energy storage systems usually include batteries and flywheels [2].The storing device in the microgrid is equivalent to the rotating reserve of large generators in the conventional grid which ensures the balance between energy generation and consumption especially during rapid changes in load or generation [3].

From the customer point of view, microgrids deliver both thermal and electricity requirements and in addition improve local reliability, reduce emissions, improve power excellence by supportive voltage and reducing voltage dips and potentially lower costs of energy supply. From the utility viewpoint, application of distributed energy sources can potentially reduce the demand for distribution and transmission facilities. Clearly, distributed generation located close to loads will reduce flows in transmission and distribution circuits with two important effects: loss reduction and ability to potentially substitute for network assets. In addition, the presence of generation close to demand could increase service quality seen by end customers. Microgrids can offer network support during the time of stress by relieving congestions and aiding restoration after faults. The development of microgrids can contribute to the reduction of emissions and the mitigation of climate changes. This is due to the availability and developing technologies for distributed generation units are based on renewable sources and micro sources that are characterized by very low emissions [4].

There are various advantages offered by microgrids to end-consumers, utilities and society, such as: improved energy efficiency, minimized overall energy consumption, reduced greenhouse gases and pollutant emissions, improved service quality and reliability, cost efficient electricity infrastructure replacement [2].

Technical challenges linked with the operation and controls of microgrids are immense. Ensuring stable operation during network disturbances, maintaining stability and power quality in the islanding mode of operation necessitates the improvement of sophisticated control strategies for microgrid's inverters in order to provide stable frequency and voltage in the presence of arbitrarily varying loads [4]. In light of these, the microgrid concept has stimulated many researchers and attracted the attention of governmental organizations in Europe, USA and Japan. Nevertheless, there are various technical issues associated with the integration and operation of microgrids.

1.1.2. Technical challenges in microgrid

Protection system is one of the major challenges for microgrid which must react to both main grid and microgrid faults. The protection system should cut off the microgrid from the main grid as rapidly as necessary to protect the microgrid loads for the first case and for the second case the protection system should isolate the smallest part of the microgrid when clears the fault [30]. A segmentation of microgrid, i.e. a design of multiple islands or sub-microgrids must be supported by microsource and load controllers. In these conditions problems related to selectivity (false, unnecessary tripping) and sensitivity (undetected faults or delayed tripping) of protection system may arise. Mainly, there are two main issues concerning the protection of microgrids, first is related to a number of installed DER units in the microgrid and second is related to an availability of a sufficient level of short-circuit current in the islanded operating mode of microgrid since this level may substantially drop down after a disconnection from a stiff main grid. In [30] the authors have made short-circuit current calculations for radial feeders with DER and studied that short-circuit currents which are used in over-current (OC) protection relays depend on a connection point of and a feed-in power from DER. The directions and amplitudes of short circuit currents will vary because of these conditions. In reality the operating conditions of microgrid are persistently varying because of the intermittent microsources (wind and solar) and periodic load variation. Also the network topology can be changed frequently which aims to minimize loss or to achieve other economic or operational targets. In addition controllable islands of different size and content can be formed as a result of faults in the main grid or inside microgrid. In such

situations a loss of relay coordination may happen and generic OC protection with a single setting group may become insufficient, i.e. it will not guarantee a selective operation for all possible faults. Hence, it is vital to ensure that settings chosen for OC protection relays take into account a grid topology and changes in location, type and amount of generation. Otherwise, unwanted operation or failure may occur during necessary condition. To deal with bi-directional power flows and low short-circuit current levels in microgrids dominated by microsources with power electronic interfaces a new protection philosophy is essential, where setting parameters of relays must be checked/updated periodically to make sure that they are still appropriate.

1.2. Literature review

The popularity of distributed generation systems is growing faster from last few years because of their higher operating efficiency and low emission levels. Distributed generators make use of several microsources for their operation like photovoltaic cells, batteries, micro turbines and fuel cells. During peak load hours DGs provide peak generation when the energy cost is high and stand by generation during system outages. Microgrid is built up by combining cluster of loads and parallel distributed generation systems in a certain local area. Microgrids have large power capacity and more control flexibility which accomplishes the reliability of the system as well as the requirement of power quality. Operation of microgrid needs implementation of high performance power control and voltage regulation algorithm [1]-[5].

To realize the emerging potential of distributed generation, a system approach i.e. microgrid is proposed which considers generation and associated loads as a subsystem. This approach involves local control of distributed generation and hence reduces the need for central dispatch. During disturbances by islanding generation and loads, local reliability can be higher in microgrid than the whole power system. This application makes the system efficiency double. The current implementation of microgrid incorporates sources with loads, permits for intentional islanding and use available waste heat of power generation systems [6].

Microgrid operates as a single controllable system which offers both power and heat to its local area. This concept offers a new prototype for the operation of distributed generation. To the utility microgrid can be regarded as a controllable cell of power system. In case of faults in microgrid, the main utility should be isolated from the distribution section as fast as

necessary to protect loads. The isolation depends on customer's load on the microgrid. Sag compensation can be used in some cases with isolation from the distribution system to protect the critical loads [2].

The microgrid concept lowers the cost and improves the reliability of small scale distributed generators. The main purpose of this concept is to accelerate the recognition of the advantage offered by small scale distributed generators like ability to supply waste heat during the time of need. From a grid point of view, microgrid is an attractive option as it recognizes that the nation's distribution system is extensive, old and will change very slowly. This concept permits high penetration of distribution generation without requiring redesign of the distribution system itself [7].

The microgrid concept acts as solution to the problem of integrating large amount of micro generation without interrupting the utility network's operation. The microgrid or distribution network subsystem will create less trouble to the utility network than the conventional micro generation if there is proper and intelligent coordination of micro generation and loads. In case of disturbances on the main network, microgrid could potentially disconnect and continue to operate individually, which helps in improving power quality to the consumer [8].

With advancement in DGs and microgrids there is development of various essential power conditioning interfaces and their associated control for tying multiple microsources to the microgrid, and then tying the microgrids to the traditional power systems. Microgrid operation becomes highly flexible, with such interconnection and can be operated freely in the grid connected or islanded mode of operation. Each microsource can be operated like a current source with maximum power transferred to the grid for the former case. The islanded mode of operation with more balancing requirements of supply-demand would be triggered when the main grid is not comparatively larger or is simply disconnected due to the occurrence of a fault. Without a strong grid and a firm system voltage, each microsource must now regulate its own terminal voltage within an allowed range, determined by its internally generated reference. The microsource thus appears as a controlled voltage source, whose output should rightfully share the load demand with the other sources. The sharing should preferably be in proportion to their power ratings, so as not to overstress any individual entity [9].

The installation of distributed generators involves technical studies of two major fields. First one is the dealing with the influences induced by distributed generators without making large modifications to the control strategy of conventional distribution system and the other one is generating a new concept for utilization of distributed generators. The concept of the microgrid follows the later approach. There includes several advantages with the installation of microgrid. Efficiently microgrid can integrate distributed energy resources with loads. Microgrid considered as a 'grid friendly entity" and does not give undesirable influence to the connecting distribution network i.e. operation policy of distribution grid does not have to be modified. It can also operate independently in the occurrence of any fault. In case of large disturbances there is possibility of imbalance of supply and demand as microgrid does not have large central generator. Also microgrid involves different DERs. Even if energy balance is being maintained there continues undesirable oscillation [10].

For each component of the microgrid, a peer-to-peer and plug-and-play model is used to improve the reliability of the system. The concept of peer-to-peer guarantees that with loss of any component or generator, microgrid can continue its operation. Plug-and-play feature implies that without re-engineering the controls a unit can be placed at any point on the electrical system thereby helps to reduce the possibilities of engineering errors [11].

The economy of a country mainly depends upon its electric energy supply which should be secure and with high quality. The necessity of customer's for power quality and energy supply is fulfilled by distributed energy supply. The distribution system mainly includes renewable energy resources, storage systems small size power generating systems and these are normally installed close to the customer's premises. The benefits of the DERs include power quality with better supply, higher reliability and high efficiency of energy by utilization of waste heat. It is an attractive option from the environmental considerations as there is generation of little pollution. Also it helps the electric utility by reducing congestion on the grid, reducing need for new generation and transmission and services like voltage support and demand response. Microgrid is an integrated system. The integration of the DERs connected to microgrid is critical. Also there is additional problem regarding the control and grouping and control of DERs in an efficient and reliable manner [12].

Integration of wind turbines and photovoltaic systems with grid leads to grid instability. One of the solutions to this problem can be achieved by the implementation of microgrid. Even though there are several advantages associated with microgrid operation, there are high transmission line losses. In a microgrid there are several units which can be utilized in a

house or country. In a house renewable energy resources and storage devices are connected to DC bus with different converter topology from which DC loads can get power supply. Inverters are implemented for power transfer between AC and DC buses. Common and sensitive loads are connected to AC bus having different coupling points. During fault in the utility grid microgrid operates in islanded mode. If in any case renewable source can't supply enough power and state of charge of storage devices are low microgrid disconnects common loads and supply power to the sensitive loads [13].

Renewable energy resources are integrated with microgrid to reduce the emission of CO_2 and consumption of fuel. The renewable resources are very fluctuant in nature, and also the production and consumption of these sources are very difficult. Therefore new renewable energy generators should be designed having more flexibility and controllability [14].

In conventional AC power systems AC voltage source is converted into DC power using an AC/DC inverter to supply DC loads. AC/DC/AC converters are also used in industrial drives to control motor speed. Because of the environmental issues associated with conventional power plant renewable resources are connected as distributed generators or ac microgrids. Also more and more DC loads like light emitting diode lights and electric vehicles are connected to AC power systems to save energy and reduce carbon dioxide (CO_2)emission. Long distance high voltage transmission is no longer necessary when power can be supplied by local renewable power sources. AC sources in a DC grid have to be converted into DC and AC loads connected into DC grid using DC/AC inverters [15].

DC systems use power electronic based converters to convert AC sources to DC and distribute the power using DC lines. DC distribution becomes attractive for an industrial park with heavy motor controlled loads and sensitive electronic loads. The fast response capability of these power electronic converters help in providing highly reliable power supply and also facilitate effective filtering against disturbances. The employment of power electronic based converters help to suppress two main challenges associated with DC systems as reliable conversion from AC/DC/AC and interruption of DC current under normal as well as fault condition [16]. Over a conventional AC grid system, DC grid has the advantage that power supply connected with the DC grid can be operated cooperatively because DC load voltage are controlled. The DC grid system operates in stand-alone mode in the case of the abnormal or fault situations of AC utility line, in which the generated power is supplied to the loads connected with the DC grid. Changes in the generated power and the load consumed power

can be compensated as a lump of power in the DC gird. The system cost and loss reduce because of the requirement of only one AC grid connected inverter [17].

Therefore the efficiency is reduced due to multistage conversions in an AC or a DC grid. So to reduce the process of multiple DC/AC/DC or AC/DC/AC conversions in an individual AC or DC grid, hybrid AC/DC microgrid is proposed, which also helps in reducing the energy loss due to reverse conversion [15].

Mostly renewable power plants are implemented in rural areas which are far away from the main grid network and there is possibility of weak transmission line connection. The microgrid (MG) concept provides an effective solution for such weak systems. The operation can be smoothened by the hybrid generation technologies while minimizing the disturbances due to intermittent nature of energy from PV and wind generation. Also there is possibility of power exchange with the main grid when excess/shortage occurs in the microgrid [18].

Distributed generation is gaining more popularity because of their advantages like environmental friendliness, expandability and availability without making any alternation to the existing transmission and distribution grid. Modern sources depend upon environmental and climatic conditions hence make them uncontrollable. Because of this problem microgrid concept comes into feature which cluster multiple distributed energy resources having different operating principles. In grid tied mode distributed green sources operates like controlled current source with surplus energy channeled by the mains to other distant loads. There is need of continuous tuning of source outputs which can be achieved with or without external communication links. In case of any malfunctions grid tied mode is proved less reliable as this leads to instability [19].

1.3. Motivation of project work

The microgrid concept acts as a solution to the conundrum of integrating large amounts of micro generation without disrupting the operation of the utility network. With intelligent coordination of loads and micro-generation, the distribution network subsystem (or 'microgrid') would be less troublesome to the utility network, than conventional microgeneration. The net microgrid could even provide ancillary services such as local voltage control. In case of disturbances on the main network, microgrids could potentially disconnect and continue to operate separately. This operation improves power quality to the customer. From the grid's perception, the benefit of a microgrid is that it can be considered as a controlled entity within the power system that can be

functioned as a single aggregated load. Customers can get benefits from a microgrid because it is designed and operated to meet their local needs for heat and power as well as provide uninterruptible power, enhance local reliability, reduce feeder losses, and support local voltages/correct voltage sag. In addition to generating technologies, microgrid also includes storage, load control and heat recovery equipment. The ability of the microgrid to operate when connected to the grid as well as smooth transition to and from the island mode is another important function.

1.4. Objective of the thesis

The main **objective** of this thesis is the development of a hybrid microgrid which will reduce the process of multiple reverse conversions associated with individual AC and DC grid by the combination of

- AC and DC sub-grid
- Photovoltaic (PV) system and
- Wind turbine generator

In order to analyze the operation of microgrid system both the modeling and controlling of the system are important issues. Hence the control and modeling (to be discussed detail in Chapter 4) are also the part of this thesis work. As a part of the thesis work the overall system is simulated using MATLAB environment. In simulation work the system is modeled using different state equations.

1.5. Thesis organization

The thesis has been organized into six chapters. Following the chapter on introduction, the rest of the thesis is outlind as follows.

Chapter 2 explains detailed modeling of PV array with the implantation of maximum power point tracking. Also the battery model is studied.

Chapter 3 represents explains the modeling of the overall DFIG system in detail. In this chapter the detail explanation is made using block diagrams and different algebraic equations.

In chapter 4 the overall configuration of the hybrid microgrid system was implemented. Along with the operation of the grid and modeling and control of the used converters are described.

Chapter 5 presents all the simulation results which are found using MATLAB/ SIMULINK environment.

Chapter 6 provides comprehensive summary and conclusions of the work undertaken in this thesis and also acknowledge about the future work. The references taken for the purpose of research work are also the part of this chapter.

CHAPTER 2

PHOTOVOLTAIC SYSTEM AND BATTERY

2.1. Photovoltaic system

The photoelectric effect was first noted by French physicist Edmund Becquerel in 1839. He proposed that certain materials have property of producing small amounts of electric current when exposed to sunlight. In 1905, Albert Einstein explained the nature of light and the photoelectric effect which has become the basic principle for photovoltaic technology. In 1954 the first photovoltaic module was built by Bell Laboratories.

A photovoltaic system makes use of one or more solar panels to convert solar energy into electricity. It consists of various components which include the photovoltaic modules, mechanical and electrical connections and mountings and means of regulating and/or modifying the electrical output.

2.1.1. Photovoltaic arrangements

2.1.1.1. Photovoltaic cell

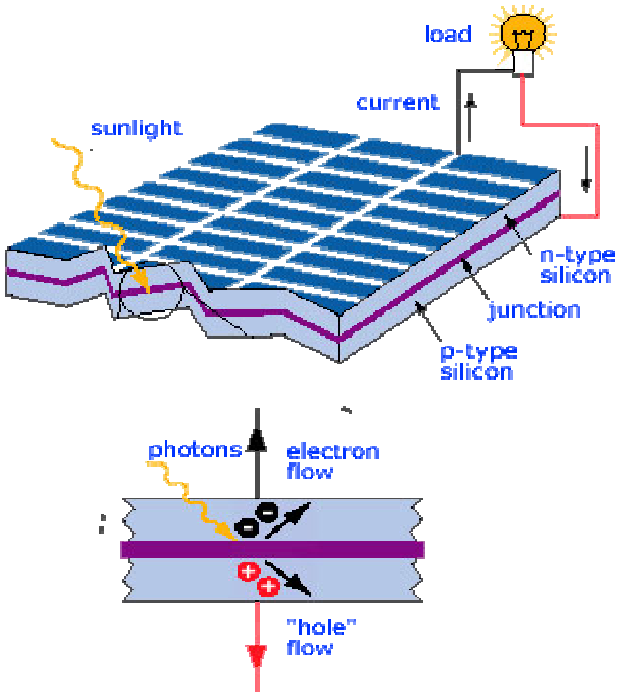

Fig 2.1. Basic structure of PV cell

The basic ingredients of PV cells are semiconductor materials, such as silicon. For solar cells, a thin semiconductor wafer creates an electric field, on one side positive and negative on the other. When light energy hits the solar cell, electrons are knocked loose from the atoms in the semiconductor material. When electrical conductors are connected to the positive and negative sides an electrical circuit is formed and electrons are captured in the form of an electric current that is, electricity. This electricity is used to power a load. A PV cell can either be circular or square in construction.

2.1.1.2. Photovoltaic module

Because of the low voltage generation in a PV cell (around 0.5V), several PV cells are connected in series (for high voltage) and in parallel (for high current) to form a PV module for desired output. In case of partial or total shading, and at night there may be requirement of separate diodes to avoid reverse currents The p-n junctions of mono-crystalline silicon cells may have adequate reverse current characteristics and these are not necessary. There is wastage of power because of reverse currents which directs to overheating of shaded cells. At higher temperatures solar cells provide less efficiency and installers aim to offer good ventilation behind solar panel. Usually there are of 36 or 72 cells in general PV modules. The modules consist of transparent front side, encapsulated PV cell and back side. The front side is usually made up of low-iron and tempered glass material. The efficiency of a PV module is less than a PV cell. This is because of some radiation is reflected by the glass cover and frame shadowing etc.

2.1.1.3. Photovoltaic array

A photovoltaic array (PV system) is an interconnection of modules which in turn is made up of many PV cells in series or parallel. The power produced by single module is not enough to meet the requirements of commercial applications, so modules are connected to form array to supply the load. In an array the connection of the modules is same as that of cells in a module. The modules in a PV array are usually first connected in series to obtain the desired voltages; the individual modules are then connected in parallel to allow the system to produce more current. In urban uses, generally the arrays are mounted on a rooftop. PV array output can directly feed to a DC motor in agricultural applications.

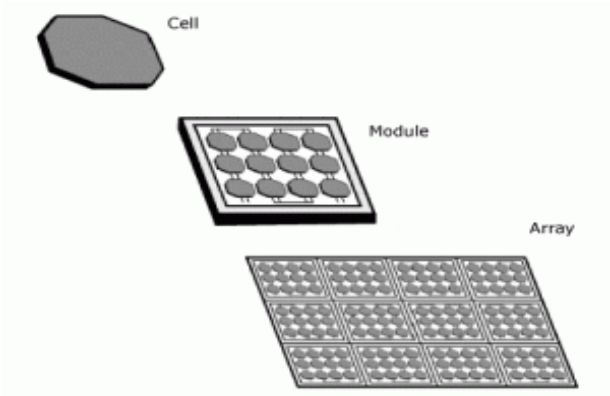

Fig 2.2. Photovoltaic system

2.1.2. Working of PV cell

The basic principle behind the operation of a PV cell is photoelectric effect. In this effect electron gets ejected from the conduction band as a result of the absorption of sunlight of a certain wavelength by the matter (metallic or non-metallic solids, liquids or gases). So, in a photovoltaic cell, when sunlight hits its surface, some portion of the solar energy is absorbed in the semiconductor material.

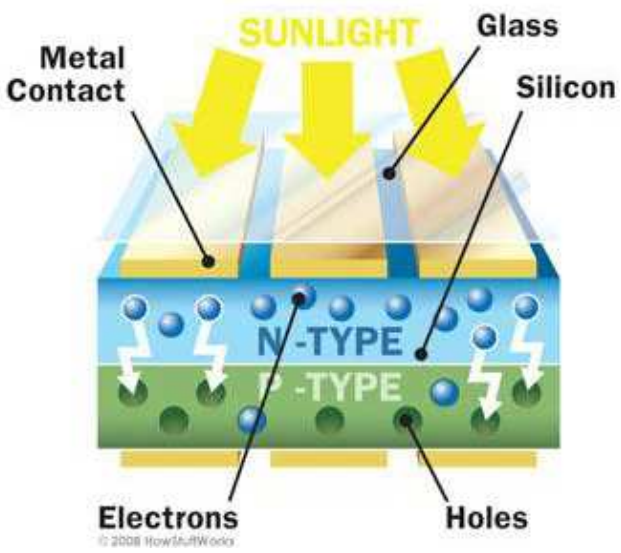

Fig 2.3. Working of PV cell

The electron from valence band jumps to the conduction band when absorbed energy is greater than the band gap energy of the semiconductor. By these hole-electrons pairs are created in the illuminated region of the semiconductor. The electrons created in the conduction band are now free to move. These free electrons are enforced to move in a particular direction by the action of electric field present in the PV cells. These electrons

flowing comprise current and can be drawn for external use by connecting a metal plate on top and bottom of PV cell. This current and the voltage produces required power.

2.1.3. Modeling of PV panel

The photovoltaic system can generate direct current electricity without environmental impact when is exposed to sunlight. The basic building block of PV arrays is the solar cell, which is basically a p-n junction that directly converts light energy into electricity. The output characteristic of PV module depends on the cell temperature, solar irradiation, and output voltage of the module. The figure shows the equivalent circuit of a PV array with a load [20].

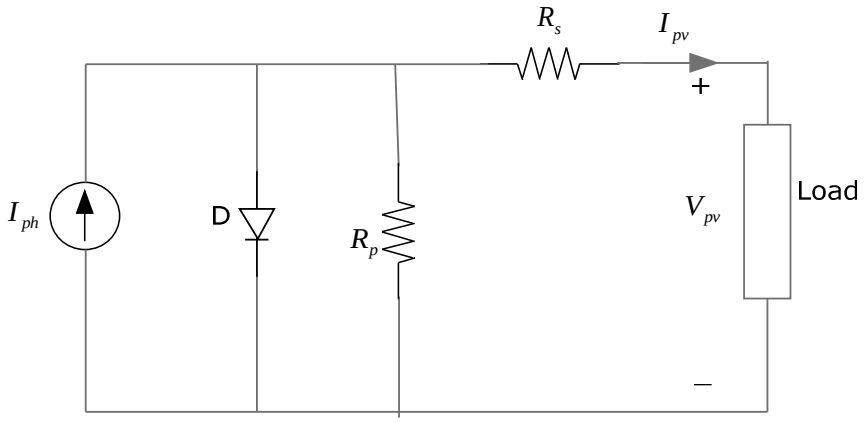

Fig 2.4. Equivalent circuit of a solar cell

Usually the equivalent circuit of a general PV model consists of a photocurrent, a diode, a parallel resistor which expresses a leakage current, and a series resistor which describes an internal resistance to the current flow. The voltage current characteristic equation of a solar cell is given as

$$I_{pv} = I_{PH} - I_S[\exp(q(V_{pv} + I_{pv}R_S)/kT_CA) - 1] - (V_{pv} + I_{pv}R_S)/R_P \quad (2.1)$$

The photocurrent mainly depends on the cell's working temperature and solar irradiation, which is explained as

$$I_{PH} = [I_{SC} + K_I(T_C - T_{Ref})]\lambda/1000 \quad (2.2)$$

The saturation current of the cell varies with the cell temperature, which is represented as

$$I_S = I_{RS}(T_C/T_{Ref})^3 \exp[qE_G(1/T_{Ref} - 1/T_C)/kA] \quad (2.3)$$

The shunt resistance R_P of the cell is inversely related with shunt leakage current to the ground. Usually efficiency of PV array is insensitive to variation in R_P and the shunt-leakage resistance can be assumed to approach infinity without leakage current to ground.

Alternatively a small variation in series resistance R_S will significantly affect output power of the PV cell. The appropriate model of PV solar cell with suitable complexity is shown in Fig.2.4. Equation (2.1) can be modified to be

$$I_{pv} = I_{PH} - I_S[\exp(q(V_{pv} + I_{pv}R_S)/kT_CA) - 1] \quad (2.4)$$

There is no series loss and no leakage to ground for an ideal PV cell, i.e., $R_S = 0$ and $R_P = \infty$. So equation (2.1) can be rewritten as

$$I_{pv} = I_{PH} - I_S[\exp(qV_{pv}/kT_CA) - 1] \quad (2.5)$$

A PV array is a group of several PV modules which are electrically connected in series and parallel circuits to generate the required current and voltage. So the current and voltage equation of the array with N_P parallel and N_S series cells can be represented as

$$I_{pv} = N_PI_{PH} - N_PI_S[\exp(q(V_{pv}/N_S + I_{RS}/N_P)/kT_CA) - 1] - (N_PV_{pv}/N_S + I_{RS})/R_P \quad (2.6)$$

The efficiency of a PV cell is sensitive to small change in series resistance but insensitive to variation in shunt resistance. The role of series resistance is very important for a PV module and the shunt resistance is approached to be infinity which can also be assumed as open. The mathematical equation of the model can be described by considering series and parallel resistance as

$$I_{pv} = N_PI_{PH} - N_PI_S[\exp(q(V_{pv}/N_S + I_{pv}R_S/N_P)/kT_CA) - 1] \quad (2.7)$$

The equation (2.7) can be simplified as

$$I_{pv} = N_PI_{PH} - N_PI_S[\exp(qV_{pv}/N_SkT_CA) - 1] \quad (2.8)$$

The open-circuit voltage V_{OC} and short-circuit current I_{SC} are the two most important parameters used which describes the cell electrical performance. The above mentioned equations are implicit and nonlinear; hence, it is not easy to arrive at an analytical solution for the specific temperature and irradiance. Normally $I_{PH} \gg I_S$, so by neglecting the small diode and ground-leakage currents under zero-terminal voltage, the short-circuit current is approximately equal to the photocurrent, i.e.

$$I_{PH} = I_{SC} \quad (2.9)$$

The open-circuit voltage parameter is obtained by assuming the zero output current. With the given open-circuit voltage at reference temperature and ignoring the shunt-leakage current, the reverse saturation current can be acquired as

$$I_{RS} = I_{SC}/[\exp(qV_{OC}/N_S kAT_C) - 1] \quad (2.10)$$

Additionally, the maximum power can be stated as

$$P_{max} = V_{max} I_{max} = \gamma V_{OC} I_{SC} \quad (2.11)$$

The parameters used for the modeling of photovoltaic panel are shown in the table 2.1 [16].

Symbol	Value
V_{OC}	403 V
q	1.602×10^{-19}C
k	1.38×10^{-23} K
A	1.50
I_{SC}	3.27 A
K_I	1.7×10^{-3}
T_{Ref}	301.18 K
I_{RS}	2.0793×10^{-6} A
T_C	350 K
λ	0-1500 W/m^2
N_P	40
N_s	900
E_G	1.1 eV

Table 2.1. Parameters for photovoltaic panel

2.2. Maximum power point tracking

As an electronic system maximum power point tracker (MPPT) functions the photovoltaic (PV) modules in a way that allows the PV modules to produce all the power they are capable of. It is not a mechanical tracking system which moves physically the modules to make them point more directly at the sun. Since MPPT is a fully electronic system, it varies the module's operating point so that the modules will be able to deliver maximum available power. As the outputs of PV system are dependent on the temperature, irradiation, and the load characteristic MPPT cannot deliver the output voltage perfectly. For this reason MPPT is required to be implementing in the PV system to maximize the PV array output voltage.

2.2.1. Necessity of maximum power point tracking

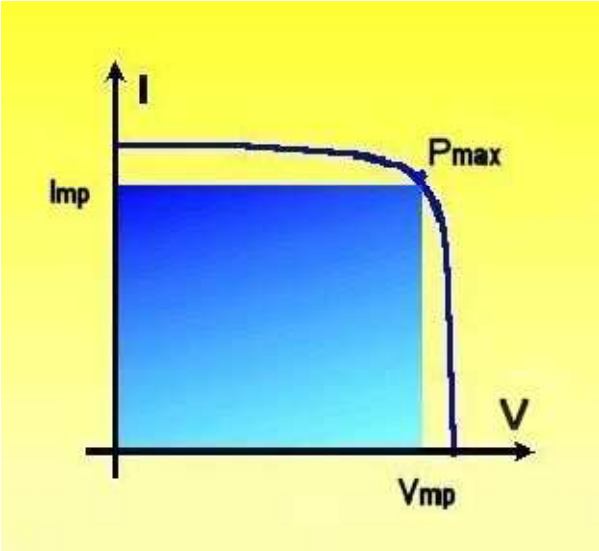

Fig 2.5. MPP characteristic

In the power versus voltage curve of a PV module there exists a single maxima of power, i.e. there exists a peak power corresponding to a particular voltage and current. The efficiency of the solar PV module is low about 13%. Since the module efficiency is low it is desirable to operate the module at the peak power point so that the maximum power can be delivered to the load under varying temperature and irradiation conditions. This maximized power helps to improve the use of the solar PV module. A maximum power point tracker (MPPT) extracts maximum power from the PV module and transfers that power to the load. As an interfacing device DC/DC converter transfers this maximum

power from the solar PV module to the load. By changing the duty cycle, the load impedance is varied and matched at the point of the peak power with the source so as to transfer the maximum power.

2.2.2. Algorithms for tracking of maximum power point

There are different algorithms which help to track the peak power point of the solar PV module automatically. The algorithms can be written as

a. Perturb and observe

b. Incremental conductance

c. Parasitic capacitance

d. Voltage based peak power tracking

e. Current Based peak power tracking

2.2.2.1. Perturb and observe

In this algorithm a slight perturbation is introduced in the system. The power of the module changes due to this perturbation. If the power increases due to the perturbation then the perturbation is continued in that direction. When power attains its peak point, the next instant power decreases and so also the perturbation reverses. During the steady state condition the algorithm oscillates around the peak point. The perturbation size is kept very small to keep the power variation small. It is examined that there is some power loss because of this perturbation and also it fails to track the power under fast varying atmospheric conditions. But still this algorithm is very popular and simple [22], [23].

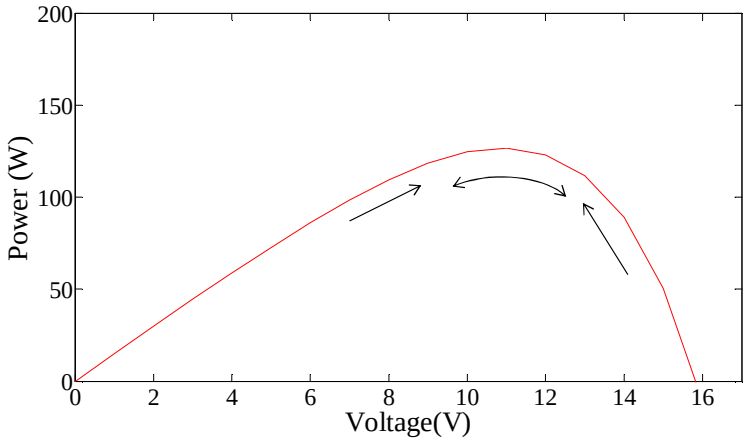

Fig 2.6. Perturb and observe algorithm

In the present work this algorithm is chosen. Figure 2.7 represents the flow chart of the algorithm. The algorithm observes output power of the array and perturbs the power based on increment of the array voltage. The algorithm continuously increments or decrements the reference voltage based on the value of the previous power sample.

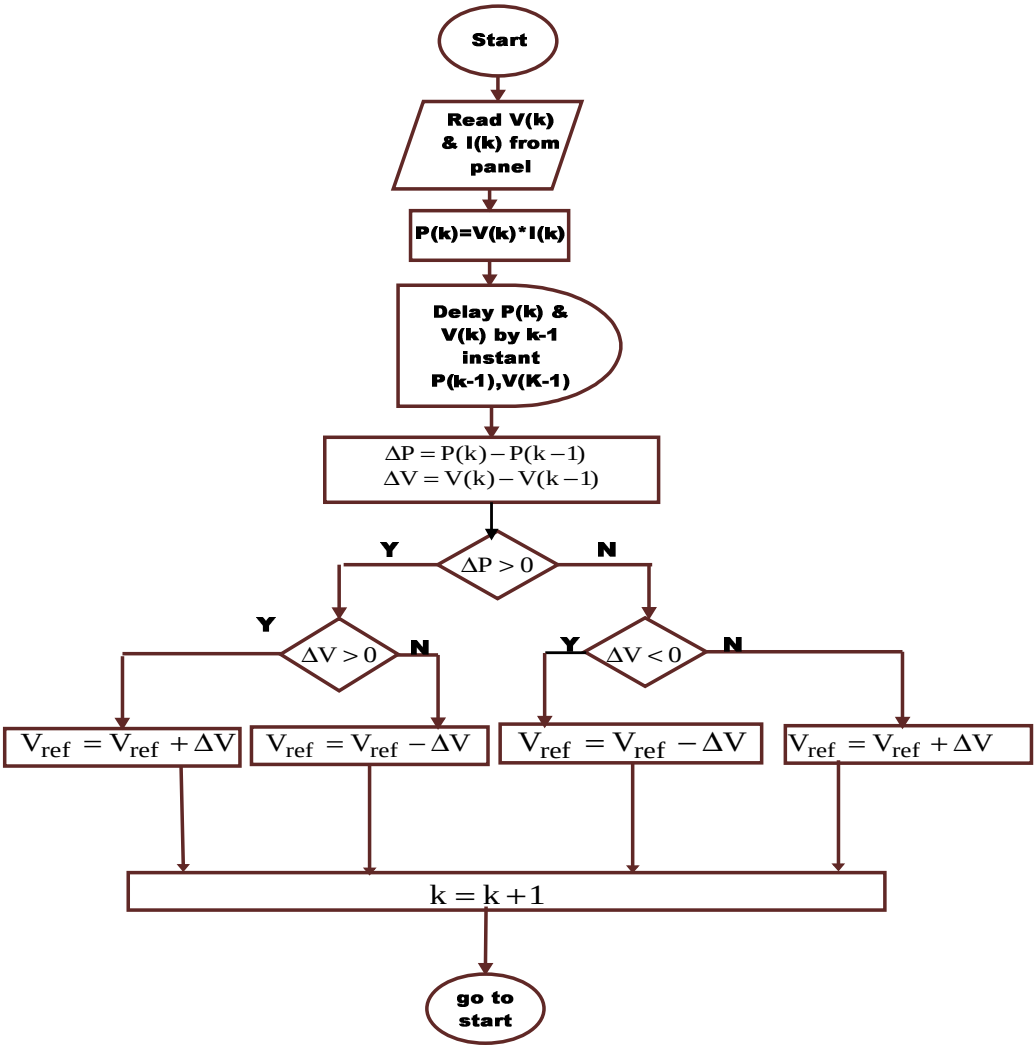

Fig 2.7. Flowchart Perturb and observe algorithm

Here a reference voltage V_{ref} is set corresponding to the peak power point of the module. The value of current and voltage can be obtained from the solar PV module. From the measured voltage and current power is calculated. The value of voltage and power at k^{th} instant are stored. Then values at $(k+1)^{th}$ instant are measured again and power is calculated from the measured values. The power and voltage at $(k+1)^{th}$ instant are subtracted with the values from k^{th} instant. If we observe the power voltage curve of the solar PV module we see that in the right hand side curve where the voltage is almost constant

the slope of power voltage is negative $\left(^{dP}/_{dV} < 0\right)$ where as in the left hand side the slope is positive $\left(^{dP}/_{dV} > 0\right)$. Depending on the sign of dP[P(k + 1) − P(k)] and dV[V(k + 1) − V(k)] after subtraction the algorithm decides whether to increase or to reduce the reference voltage.

The P&O method is claimed to have slow dynamic response and high steady state error. In fact, the dynamic response is low when a small increment value and a low sampling rate are employed. To decrease the steady state error low increments are essential because the P&O always makes the operating point oscillate near the MPP, but never at the MPP exactly. When the increment is lower, the system will be closer to the array MPP. In case of greater increment, the algorithm will work faster, but the steady state error will be increased. The small increments tend to make the algorithm more stable and accurate when the operating conditions of the PV array change. In case of large increments the algorithm becomes confused since the response of the converter to large voltage or current variations will cause oscillations, overshoot and the settling time of the converter itself confuse the algorithm [24].

2.2.2.2. Incremental conductance

The incremental conductance method can overwhelm the problems of tracking peak power under fast varying atmospheric condition [22], [23].

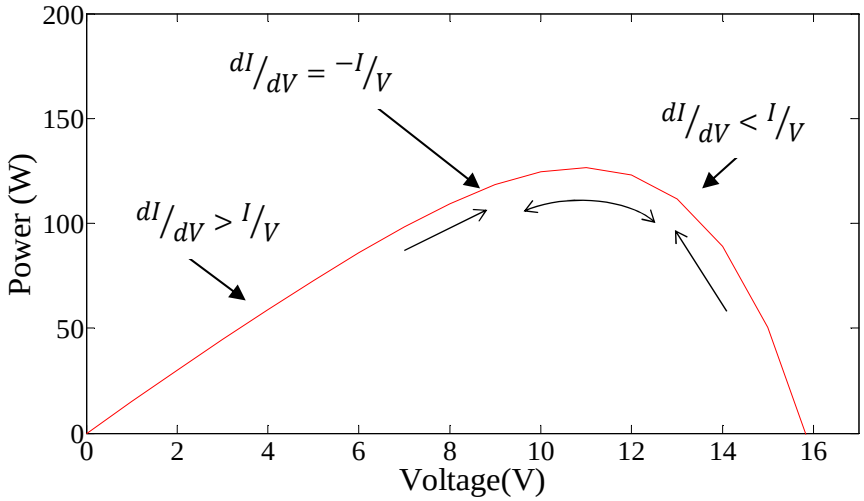

Fig 2.8. Incremental conductance algorithm

The algorithm uses the equation

$$P = V * I \tag{2.12}$$

(Where P=power of the module, V= voltage of the module, I= current of the module);

Differentiating with respect to dV

$$dP/dV = I + dI/dV \quad (2.13)$$

The algorithm works depending on this equation.

At peak power point

$$dP/dV = 0 \quad (2.14)$$

$$dI/dV = -I/V \quad (2.15)$$

If the operating point is to the right of the power curve then we have

$$dP/dV < 0 \quad (2.16)$$

$$dI/dV < I/V \quad (2.17)$$

If operating point is to the left of the power curve then we have

$$dP/dV > 0 \quad (2.18)$$

$$dI/dV > I/V \quad (2.19)$$

The algorithm works using equations (2.15), (2.17), & (2.18).

When the incremental conductance decides that the MPPT has reached the MPP, it stops perturbing the operating point. If this condition is not achieved, MPPT operating point direction can be computed using dI/dV and $-I/V$ relation. This relationship is derived from the fact that when the MPPT is to the right of the MPP dP/dV is negative and positive when it is to the left of the MPP. This algorithm has benefits over perturb and observe in that it can determine when the MPPT has reached the MPP, where perturb and observe oscillates around the MPP. Also, this algorithm can track rapidly increasing and decreasing irradiance conditions with higher accuracy than perturb and observe. The drawback of this algorithm is that there is increased complexity when compared to perturb and observe.

2.2.2.3. Parasitic capacitances

The improvement of the incremental conductance leads to the method of parasitic capacitance which considers the parasitic capacitances of the solar cells. This method makes use of the switching ripple of the MPPT which helps to perturb the array. The average ripple in the PV array voltage and power, generated by the switching frequency are measured

using a series of filters and multipliers and then used to calculate the array conductance. Then the algorithm decides the direction of movement of MPPT operating point. There is one disadvantage in this algorithm that the parasitic capacitance in each module is very small, and can perform well in large PV arrays where several PV modules are connected in parallel. There is sizable input capacitor in the DC-DC converter which filters out small ripple in the array power. This capacitor may cover the overall effects of the parasitic capacitance of the PV array [23].

2.2.2.4. Voltage control maximum power point tracker

The maximum power point (MPP) of a PV module is assumed to lie about 0.75 times the open circuit voltage of the module. Hence a reference voltage can be generated by calculating the open circuit voltage and then the feed forward voltage control scheme can be implemented to bring the solar PV module voltage to the point of maximum power. The difficulty associated with this technique is that there is variation of open circuit voltage with the temperature. As there is increase in temperature because of the change in open circuit voltage of the module, module's open circuit is needed to be calculated frequently. In this process the load must be disconnected from the module to measure open circuit voltage. So the power during that instant cannot be utilized [25].

2.2.2.5. Current control maximum power point tracker

The module's peak power lies at the point which is about 0.9 times the short circuit current of the module. The module has to be short-circuited to measure this point. After that module current is adjusted to the value by using the current mode control which is approximately 0.9 times the short circuit current. In this case a high power resistor is required which can sustain the short-circuit current. This is the problem with this algorithm. The module has to be short circuited to measure the short circuit current as it goes on varying with the changes in irradiation level [25].

2.3. Battery

In our modern society the role of batteries is important as energy carriers, because of its presence in devices for everyday use. At the end of the 20^{th} century the demand for batteries rapidly increased due to the large interest in wireless devices. Today, the battery industry comes under the category of large-scale industry which produces several million batteries per month. Improving the energy capacity is one major development issue, however, for consumer products, safety is probably considered equally important today. With the

introduction of hybrid electric vehicles into the market there is technological development in the battery field which leads to reduction of fuel consumption and gas emissions. Battery development is a major task for both industry and academic research.

2.3.1. Modeling of battery

The battery is modeled as a nonlinear voltage source whose output voltage depends not only on the current but also on the battery state of charge (SOC), which is a nonlinear function of the current and time [26]. Fig 2.9 represents a basic model of battery.

Two parameters to represent state of a battery i.e. terminal voltage and state of charge can be written as:

$$V_b = V_0 + R_b i_b - K\frac{Q}{Q - \int i_b dt} + A * \exp(B \int i_b \, dt) \quad (2.20)$$

$$SOC = 100\left(1 + \frac{\int i_b dt}{Q}\right) \quad (2.21)$$

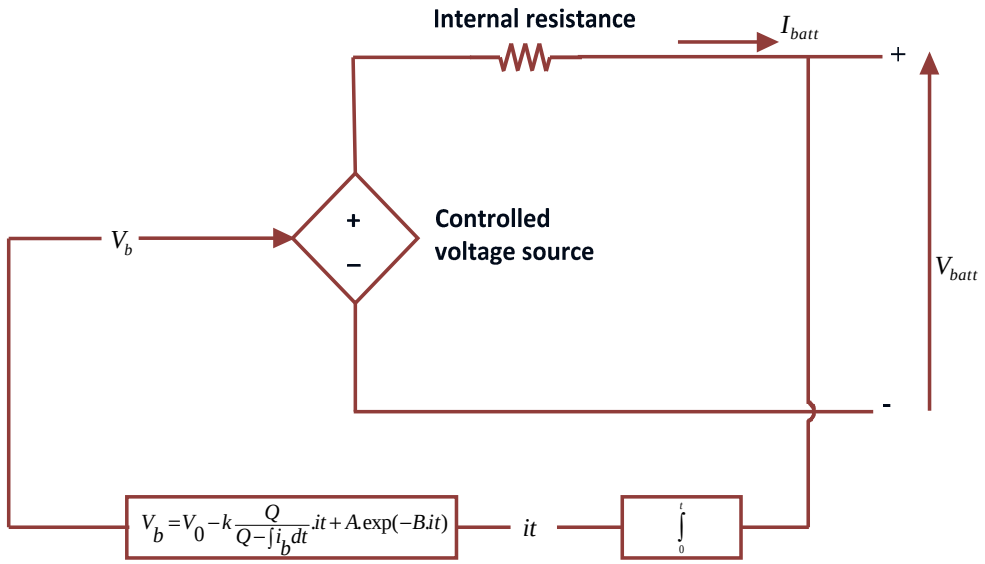

Fig 2.9. Model of battery

The original Shepherd model has a non-linear term equal to $K\frac{Q}{Q - \int i_b dt}$. This term represents a non-linear voltage that changes with the amplitude of the current and the actual charge of the battery. So when there is complete discharge of battery and no flow of current, the voltage of the battery will be nearly zero. As soon as a current circulates again, the voltage falls abruptly. This model yields accurate results and also represents the behaviour of the battery.

2.4. Summary

This chapter summarizes the modeling of solar panel with the implementation of maximum power point tracking algorithm. Various MPPT algorithms are introduced for the study of PV array to track maximum power under various solar irradiation and temperature conditions. Also the model of battery is explained in detail for the modeling of microgrid.

CHAPTER 3

DOUBLY FED INDUCTION GENERATOR

3.1. Wind turbines

With the use of power of the wind, wind turbines produce electricity to drive an electrical generator. Usually wind passes over the blades, generating lift and exerting a turning force. Inside the nacelle the rotating blades turn a shaft then goes into a gearbox. The gearbox helps in increasing the rotational speed for the operation of the generator and utilizes magnetic fields to convert the rotational energy into electrical energy. Then the output electrical power goes to a transformer, which converts the electricity to the appropriate voltage for the power collection system. A wind turbine extracts kinetic energy from the swept area of the blades.

The power contained in the wind is given by the kinetic energy of the flowing air mass per unit time [28]. The equation for the power contained in the wind can then be written as

$$P_{air} = \frac{1}{2}(\text{air mass per unit time})(V_\infty)^2$$

$$= \frac{1}{2}(\rho A V_\infty)(V_\infty)^2$$

$$= \frac{1}{2}\rho A {V_\infty}^3 \quad (3.1)$$

Although Eq. (3.1) describes the availability of power in the wind, power transferred to the wind turbine rotor is reduced by the power coefficient C_p.

$$C_p = \frac{P_{\text{wind turbine}}}{P_{air}} \quad (3.2)$$

A maximum value of C_p is defined by the Betz limit, which states that a turbine can never extract more than 59.3% of the power from an air stream. In reality, wind turbine rotors have maximum C_p values in the range 25-45%.

$$P_{\text{wind turbine}} = C_p \times P_{air} \quad (3.3)$$

It is also conventional to define a tip speed ratio λ as

$$\lambda = \frac{\omega R}{V_\infty} \quad (3.4)$$

3.2. DFIG system

The doubly fed induction machine is the most widely machine in these days. The induction machine can be used as a generator or motor. Though demand in the direction of motor is less because of its mechanical wear at the slip rings but they have gained their prominence for generator application in wind and water power plant because of its obvious adoptability capacity and nature of tractability. This section describes the detail analysis of overall DFIG system along with back to back PWM voltage source converters.

3.2.1. Mathematical modeling of induction generator

DFIG is a wound rotor type induction machine, its stator consists of stator frame, stator core, poly phase (3-phase) distributed winding, two end covers, bearing etc. The stator core is stack of cylindrical steel laminations which are slotted along their inner periphery for housing the 3-phase winding. Its rotor consists of slots in the outer periphery to house the windings like stator. The machine works on the principle of Electromagnetic Induction and the energy transfer takes place by means of transfer action. So the machine can represent as a transformer which is rotatory in action not stationary. This section explains the basic mathematical modeling of DFIG. In this section the machine modeling is explained by taking two phase parameters into consideration.

3.2.1.1. Modeling of DFIG in synchronously rotating frame

Fig 3.1 and 3.2 demonstrates the equivalent circuit diagram of an induction machine. The machine is signified as a two phase machine in this figure.

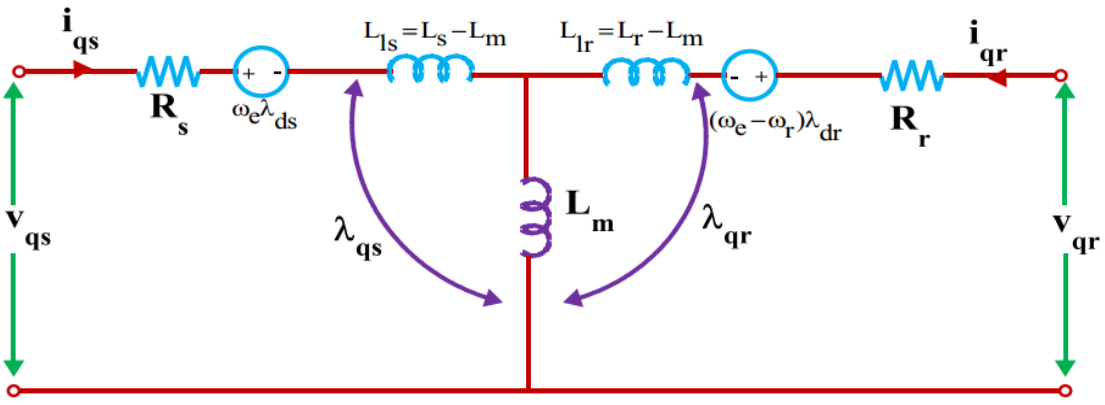

Fig 3.1. Dynamic d-q equivalent circuit of DFIG (q-axis circuit)

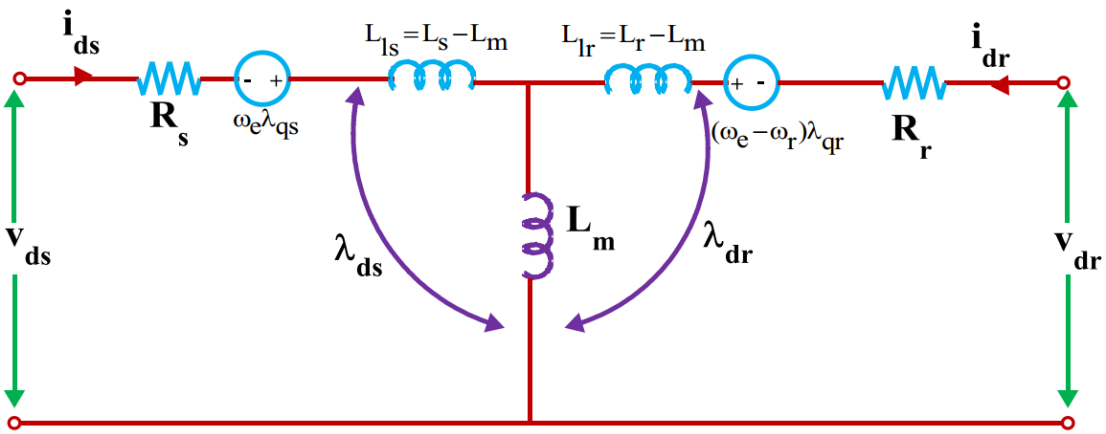

Fig 3.2. Dynamic d-q equivalent circuit of DFIG (d-axis circuit)

Equations for the stator circuit can be written as

$$v_{qs}^{s} = R_s i_{qs}^{s} + \frac{d}{dt}\lambda_{qs}^{s} \tag{3.5}$$

$$v_{ds}^{s} = R_s i_{ds}^{s} + \frac{d}{dt}\lambda_{ds}^{s} \tag{3.6}$$

In d-q frame Eq. (3.5) and (3.6) can be written [29] as

$$v_{qs} = R_s i_{qs} + \frac{d}{dt}\lambda_{qs} + (\omega_e \lambda_{ds}) \tag{3.7}$$

$$v_{ds} = R_s i_{ds} + \frac{d}{dt}\lambda_{ds} - (\omega_e \lambda_{qs}) \tag{3.8}$$

Where all the variables are in synchronously rotating frame. The bracketed terms indicate the back emf or speed emf or counter emf due to the rotation of axes as in the case of DC machines. When the angular speed ω_e is zero, the speed e.m.f due to d and q axis is zero and the equations changes to stationary form. If the rotor is blocked or not moving, i.e. $\omega_r = 0$, the machine equations can be written as

$$v_{qr} = R_r i_{qr} + \frac{d}{dt}\lambda_{qr} + (\omega_e \lambda_{dr}) \tag{3.9}$$

$$v_{dr} = R_r i_{dr} + \frac{d}{dt}\lambda_{dr} - (\omega_e \lambda_{qr}) \tag{3.10}$$

Let the rotor rotates at an angular speed ω_r, then the d-q axes fixed on the rotor fictitiously will move at a relative speed $(\omega_e - \omega_r)$ to the synchronously rotating frame.

By replacing $(\omega_e - \omega_r)$ in place of ω_e the d-q frame rotor equations can be written as

$$v_{qr} = R_r i_{qr} + \frac{d}{dt}\lambda_{qr} + (\omega_e - \omega_r)\lambda_{dr} \tag{3.11}$$

$$v_{dr} = R_r i_{dr} + \frac{d}{dt}\lambda_{dr} - (\omega_e - \omega_r)\lambda_{qr} \quad (3.12)$$

The flux linkage expressions in terms of current can be written from Fig 3.1 and 3.2 as follows:

$$\lambda_{qs} = L_{1s} i_{qs} + L_m(i_{qs} + i_{qr})$$
$$= L_m i_{qs} + L_m i_{qr} \quad (3.13)$$

$$\lambda_{ds} = L_{1s} i_{ds} + L_m(i_{ds} + i_{dr})$$
$$= L_m i_{ds} + L_m i_{dr} \quad (3.14)$$

$$\lambda_{qr} = L_{1r} i_{qr} + L_m(i_{qs} + i_{qr})$$
$$= L_r i_{qr} + L_m i_{qs} \quad (3.15)$$

$$\lambda_{dr} = L_{1r} i_{dr} + L_m(i_{ds} + i_{dr})$$
$$= L_r i_{dr} + L_m i_{ds} \quad (3.16)$$

$$\lambda_{qm} = L_m(i_{qs} + i_{qr}) \quad (3.17)$$

$$\lambda_{dm} = L_m(i_{ds} + i_{dr}) \quad (3.18)$$

Eq. (3.5) to (3.18) describes the complete electrical modeling of DFIG. Whereas Eq. (3.19) express the relations of mechanical parameters which are essential part of the modeling.

The electrical speed ω_r cannot be treated as constant in the above equations. It can be connected to the torque as

$$T_e = T_L + J\frac{d\omega_m}{dt} + B\omega_m = T_L + \frac{2}{P}J\frac{d\omega_r}{dt} + \frac{2}{P}B\omega_r \quad (3.19)$$

3.2.1.2. Dynamic modeling of DFIG in state space equations

The dynamic modeling in state space form is necessary to carried out simulation using different tools such as MATLAB. The basic sate space form helps to analyze the system in transient condition.

In the DFIG system the state variables are normally currents, fluxes etc. In the following section the state space equations for the DFIG in synchronously rotating frame has been derived with flux linkages as the state variables. As the machine and power system parameters are nearly always given in ohms or percent or per unit of base impedance, it is appropriate to

express the voltage and flux linkage equations in terms of reactances rather than inductances. The above stated voltage and flux equations can be reworked as follows:

$$v_{qs} = R_s i_{qs} + \frac{1}{\omega_b}\frac{d}{dt}\psi_{qs} + \frac{\omega_e}{\omega_b}\psi_{qs} \quad (3.20)$$

$$v_{ds} = R_s i_{ds} + \frac{1}{\omega_b}\frac{d}{dt}\psi_{ds} - \frac{\omega_e}{\omega_b}\psi_{ds} \quad (3.21)$$

$$v_{qr} = R_r i_{qr} + \frac{1}{\omega_b}\frac{d}{dt}\psi_{qr} + \frac{(\omega_e - \omega_r)}{\omega_b}\psi_{dr} \quad (3.22)$$

$$v_{dr} = R_r i_{dr} + \frac{1}{\omega_b}\frac{d}{dt}\psi_{dr} - \frac{(\omega_e - \omega_r)}{\omega_b}\psi_{qr} \quad (3.23)$$

Equations related to flux linkage i.e. Eq. (3.13)-(3.18) can be written in terms of reactances as follows:

$$\psi_{qs} = X_{ls} i_{qs} + X_m(i_{qs} + i_{qr}) \quad (3.24)$$

$$\psi_{ds} = X_{ls} i_{ds} + X_m(i_{ds} + i_{dr}) \quad (3.25)$$

$$\psi_{qr} = X_{lr} i_{qr} + X_m(i_{qs} + i_{qr}) \quad (3.26)$$

$$\psi_{dr} = X_{lr} i_{dr} + X_m(i_{ds} + i_{dr}) \quad (3.27)$$

$$\psi_{qm} = X_m(i_{qs} + i_{qr}) \quad (3.28)$$

$$\psi_{dm} = X_m(i_{ds} + i_{dr}) \quad (3.29)$$

Where reactances (X_{ls}, X_{lr}, X_m) are found by multiplying base frequency ω_b with inductances (L_{1s}, L_{1r}, L_m).

From eq. (3.24)-(3.29) we can find the expressions for currents in terms of flux linkages and also the mutual flux linkages (ψ_{qm}, ψ_{dm}) are found using current expressions.

The equations are given as follows [29].

$$i_{qs} = \frac{\psi_{qs} - \psi_{qm}}{X_{1s}} \quad (3.30)$$

$$i_{qr} = \frac{\psi_{qr} - \psi_{qm}}{X_{1r}} \quad (3.31)$$

$$i_{ds} = \frac{\psi_{ds} - \psi_{dm}}{X_{1s}} \quad (3.32)$$

$$i_{dr} = \frac{\psi_{dr} - \psi_{dm}}{X_{1r}} \quad (3.33)$$

Substituting equations (3.30)-(3.33) in (3.28)-(3.29) we get

$$\psi_{qm} = X_m\{\frac{\psi_{qs}-\psi_{qm}}{X_{1s}} + \frac{\psi_{qr}-\psi_{qm}}{X_{1r}}\}$$

$$\Longrightarrow \psi_{qm} = \frac{X_m}{X_{1s}}\psi_{qs} - \frac{X_m}{X_{1s}}\psi_{qm} + \frac{X_m}{X_{1r}}\psi_{qr} - \frac{X_m}{X_{1r}}\psi_{qm}$$

$$\Longrightarrow \psi_{qm} + \frac{X_m}{X_{1s}}\psi_{qm} + \frac{X_m}{X_{1r}}\psi_{qm} = \frac{X_m}{X_{1s}}\psi_{qs} + \frac{X_m}{X_{1s}}\psi_{qr}$$

$$\Longrightarrow \psi_{qm}\left(1 + \frac{X_m}{X_{1s}} + \frac{X_m}{X_{1r}}\right) = \frac{X_m}{X_{1s}}\psi_{qs} + \frac{X_m}{X_{1r}}\psi_{qr}$$

$$\Longrightarrow \psi_{qm}\left(\frac{X_{1s}X_r+X_mX_{1r}+X_mX_{1s}}{X_{1s}X_{1r}}\right) = \frac{X_m}{X_{1s}}\psi_{qs} + \frac{X_m}{X_{1r}}\psi_{qr}$$

$$\Longrightarrow \psi_{qm}X_m\left(\frac{X_{1s}X_r+X_mX_{1r}+X_mX_{1s}}{X_{1s}X_{1r}X_m}\right) = \frac{X_m}{X_{1s}}\psi_{qs} + \frac{X_m}{X_{1r}}\psi_{qr}$$

$$\Longrightarrow \psi_{qm}\frac{X_m}{X_{eq}} = \frac{X_m}{X_{1s}}\psi_{qs} + \frac{X_m}{X_{1r}}\psi_{qr}$$

$$\Longrightarrow \psi_{qm} = \frac{X_{eq}}{X_{1s}}\psi_{qs} + \frac{X_{eq}}{X_{1r}}\psi_{qr}$$

$$\psi_{qm} = \frac{X_{eq}}{X_{1s}}\psi_{qs} + \frac{X_{eq}}{X_{1r}}\psi_{qr} \tag{3.34}$$

Similarly we can find the value of ψ_{dm} as follows

$$\psi_{dm} = \frac{X_{eq}}{X_{1s}}\psi_{ds} + \frac{X_{eq}}{X_{1r}}\psi_{dr} \tag{3.35}$$

Substituting the current equations from (3.30)-(3.33) in voltage equations (3.20)-(3.23) we will get,

$$v_{qs} = \frac{R_s}{X_{1s}}\left(\psi_{qs} - \psi_{qm}\right) + \frac{1}{\omega_b}\frac{d\psi_{qs}}{dt} + \frac{\omega_e}{\omega_b}\psi_{ds} \tag{3.36}$$

$$v_{ds} = \frac{R_s}{X_{1s}}(\psi_{ds} - \psi_{dm}) + \frac{1}{\omega_b}\frac{d\psi_{ds}}{dt} - \frac{\omega_e}{\omega_b}\psi_{qs} \tag{3.37}$$

$$v_{qr} = \frac{R_s}{X_{1r}}\left(\psi_{qr} - \psi_{qm}\right) + \frac{1}{\omega_b}\frac{d\psi_{qr}}{dt} + \frac{(\omega_e-\omega_r)}{\omega_b}\psi_{dr} \tag{3.38}$$

$$v_{dr} = \frac{R_s}{X_{1r}}\left(\psi_{dr} - \psi_{dm}\right) + \frac{1}{\omega_b}\frac{d\psi_{dr}}{dt} - \frac{(\omega_e-\omega_r)}{\omega_b}\psi_{qr} \tag{3.39}$$

The state variables can be expressed using the above equations as follows

$$\frac{d\psi_{qs}}{dt} = \omega_b\left\{v_{qs} - \frac{\omega_e}{\omega_b}\psi_{ds} - \frac{R_s}{X_{1s}}\left(\psi_{qs} - \psi_{qm}\right)\right\} \tag{3.40}$$

$$\frac{d\psi_{ds}}{dt} = \omega_b \left\{ v_{qs} + \frac{\omega_e}{\omega_b}\psi_{qs} - \frac{R_s}{X_{1s}}\left(\psi_{ds} - \psi_{dm}\right)\right\} \tag{3.41}$$

$$\frac{d\psi_{qr}}{dt} = \omega_b \left\{ v_{qr} - \frac{(\omega_e - \omega_r)}{\omega_b}\psi_{dr} - \frac{R_r}{X_{1r}}\left(\psi_{qr} - \psi_{qm}\right)\right\} \tag{3.42}$$

$$\frac{d\psi_{dr}}{dt} = \omega_b \left\{ v_{dr} + \frac{(\omega_e - \omega_r)}{\omega_b}\psi_{qr} - \frac{R_r}{X_{1r}}\left(\psi_{dr} - \psi_{dm}\right)\right\} \tag{3.43}$$

The state space matrix can be written as follows

$$\begin{bmatrix} \dot{\psi}_{qs} \\ \dot{\psi}_{ds} \\ \dot{\psi}_{qr} \\ \dot{\psi}_{dr} \end{bmatrix} = \begin{bmatrix} -\frac{R_s}{X_{1s}} & -\frac{\omega_e}{\omega_b} & 0 & 0 \\ -\frac{\omega_e}{\omega_b} & -\frac{R_s}{X_{1s}} & 0 & 0 \\ 0 & 0 & -\frac{R_r}{X_{1r}} & -\frac{\omega_e - \omega_r}{\omega_b} \\ 0 & 0 & \frac{\omega_e - \omega_r}{\omega_b} & -\frac{R_r}{X_{1r}} \end{bmatrix} \begin{bmatrix} \psi_{qs} \\ \psi_{ds} \\ \psi_{qr} \\ \psi_{dr} \end{bmatrix} + \begin{bmatrix} 1 & 0 & 0 & 0 \\ 0 & 1 & 0 & 0 \\ 0 & 0 & 1 & 0 \\ 0 & 0 & 0 & 1 \end{bmatrix} \begin{bmatrix} v_{qs} \\ v_{ds} \\ v_{qr} \\ v_{dr} \end{bmatrix} + \begin{bmatrix} \frac{R_s}{X_{1s}} & 0 \\ 0 & \frac{R_s}{X_{1s}} \\ \frac{R_r}{X_{1r}} & 0 \\ 0 & \frac{R_r}{X_{1r}} \end{bmatrix} \begin{bmatrix} \psi_{qm} \\ \psi_{dm} \end{bmatrix} \tag{3.44}$$

The electromotive torque is developed by the interaction of air-gap flux and the rotor mmf. At synchronous speed the rotor cannot move and as a result there is no question of induced emf as well as the current, hence there is zero torque, but at any speed other than synchronous speed the machine will experience torque which is the case of motor, where as in case of generator electrical torque in terms of mechanical is provided by means of prime mover which is wind in this case.

The torque can be represented in terms of flux linkages and currents as

$$\begin{aligned} T_e &= \frac{3}{2}\frac{P}{2}\left(\lambda_{ds} i_{qs} - \lambda_{qs} i_{ds}\right) \\ &= \frac{3}{2}\frac{P}{2} L_m \left(i_{qs} i_{dr} - i_{ds} i_{qr}\right) \\ &= \frac{3}{2}\frac{P}{2}\left(\lambda_{dr} i_{qr} - \lambda_{qr} i_{dr}\right) \end{aligned} \tag{3.45}$$

Equation (3.45) can be written in terms of state variables as follows

$$\begin{aligned} T_e &= \frac{3}{2}\frac{P}{2}\frac{1}{\omega_b}\left(\psi_{ds} i_{qs} - \psi_{qs} i_{ds}\right) \\ &= \frac{3}{2}\frac{P}{2}\frac{1}{\omega_b}\left(\psi_{dr} i_{qr} - \psi_{qr} i_{dr}\right) \end{aligned} \tag{3.46}$$

Equation (3.40)-(3.46) describe the complete DFIG model in state space form, where $\psi_{qs}, \psi_{ds}, \psi_{qr}, \psi_{dr}$ are the state variables.

Symbol	Value
P_{nom}	50 kW
V_{nom}	400 V
R_s	0.00706 pu
L_s	0.171 pu
R_r	0.005 pu
L_r	0.156 pu
L_m	2.9 pu
J	3.1 s
n_p	6
V_{dc_nom}	800 V
P_m	45 kW

Table 3.1. Parameters for DFIG

The parameters used for the modeling of induction generator are shown in the table 3.1 [16].

3.3. Summary

This chapter explains the basic introduction of wind turbine. Also the detailed modeling of the doubly fed induction generator (DFIG) system is analyzed which plays a vital role in the modeling and control structure of hybrid microgrid**.**

CHAPTER 4

AC/DC MICROGRID

The concept of microgrid is considered as a collection of loads and microsources which functions as a single controllable system that provides both power and heat to its local area. This idea offers a new paradigm for the definition of the distributed generation operation. To the utility the microgrid can be thought of as a controlled cell of the power system. For example this cell could be measured as a single dispatch able load, which can reply in seconds to meet the requirements of the transmission system. To the customer the microgrid can be planned to meet their special requirements; such as, enhancement of local reliability, reduction of feeder losses, local voltages support, increased efficiency through use waste heat, voltage sag correction [3]. The main purpose of this concept is to accelerate the recognition of the advantage offered by small scale distributed generators like ability to supply waste heat during the time of need [4]. The microgrid or distribution network subsystem will create less trouble to the utility network than the conventional microgeneration if there is proper and intelligent coordination of micro generation and loads [5]. Microgrid considered as a 'grid friendly entity" and does not give undesirable influences to the connecting distribution network i.e. operation policy of distribution grid does not have to be modified [7].

4.1.Configuration of the hybrid microgrid

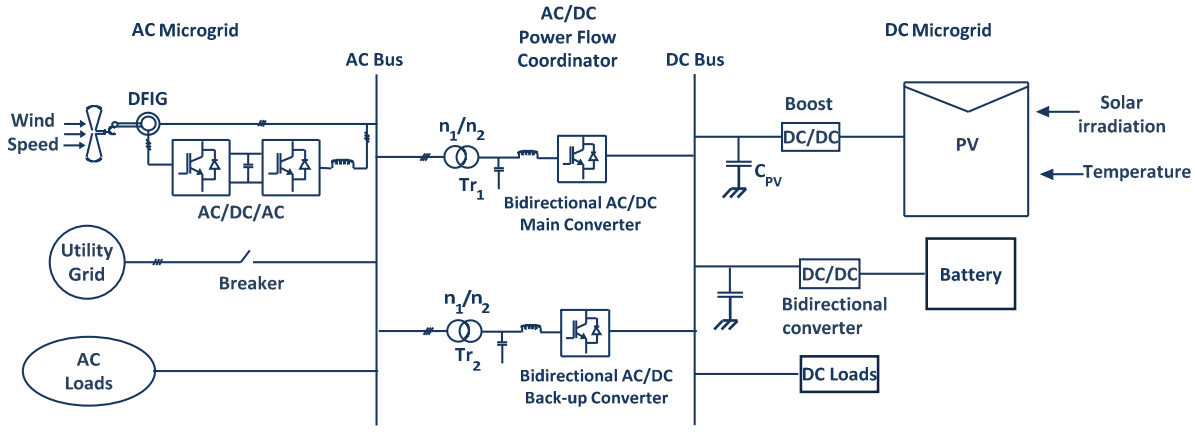

Fig 4.1. A hybrid AC/DC microgrid system

The configuration of the hybrid system is shown in Figure 1 where various AC and DC sources and loads are connected to the corresponding AC and DC networks. The AC and DC links are linked together through two transformers and two four quadrant operating three-phase converters. The AC bus of the hybrid grid is tied to the utility grid.

Figure 4.2 describes the hybrid system configuration which consists of AC and DC grid. The AC and DC grids have their corresponding sources, loads and energy storage elements, and are interconnected by a three phase converter. The AC bus is connected to the utility grid through a transformer and circuit breaker.

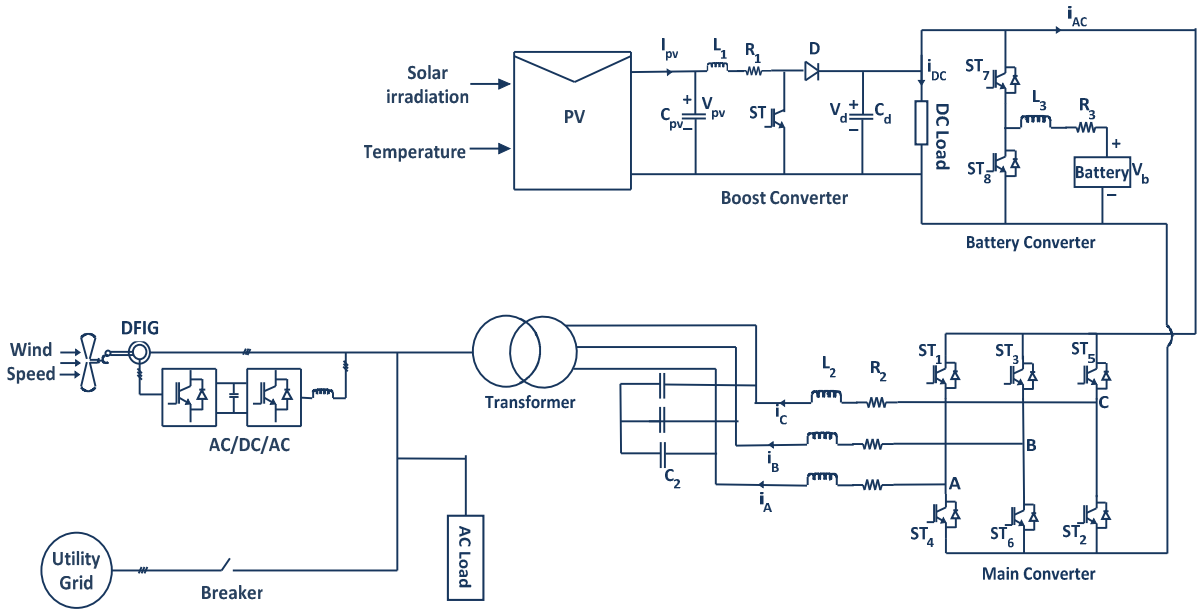

Fig 4.2. Representation of hybrid microgrid

In the proposed system, PV arrays are connected to the DC bus through boost converter to simulate DC sources. A DFIG wind generation system is connected to AC bus to simulate AC sources. A battery with bidirectional DC/DC converter is connected to DC bus as energy storage. A variable DC and AC load are connected to their DC and AC buses to simulate various loads.

PV modules are connected in series and parallel. As solar radiation level and ambient temperature changes the output power of the solar panel alters. A capacitor C_{pv} is added to the PV terminal in order to suppress high frequency ripples of the PV output voltage. The bidirectional DC/DC converter is designed to maintain the stable DC bus voltage through charging or discharging the battery when the system operates in the autonomous operation mode. The three converters (boost converter, main converter, and bidirectional converter) share a common DC bus. A wind generation system consists of doubly fed induction

generator (DFIG) with back to back AC/DC/AC PWM converter connected between the rotor through slip rings and AC bus. The AC and DC buses are coupled through a three phase transformer and a main bidirectional power flow converter to exchange power between DC and AC sides. The transformer helps to step up the AC voltage of the main converter to utility voltage level and to isolate AC and DC grids.

Symbol	Value
C_{pv}	110 µF
L_1	2.5 mH
C_d	4700 µF
L_2	0.43 mH
R_2	0.3 ohm
C_2	60 µF
L_3	3 mH
R_3	0.1 ohm
f	50 Hz
f_s	10 kHz
V_d	400 V
V_{AC_rms}	400 V

Table 4.1. Component parameters for the hybrid grid

The parameters used for the modeling of hybrid grid are show in the table 4.1 [16].

4.2.Operation of grid

The hybrid grid performs its operation in two modes.

4.2.1. Grid tied mode

In this mode the main converter is to provide stable DC bus voltage, and required reactive power to exchange power between AC and DC buses. Maximum power can be obtained by controlling the boost converter and wind turbine generators. When output power of DC sources is greater than DC loads the converter acts as inverter and in this situation power flows from DC to AC side. When generation of total power is less than the total load at DC side, the converter injects power from AC to DC side. The converter helps to inject power to the utility grid in case the total power generation is greater than the total load in the hybrid grid,. Otherwise hybrid receives power from the utility grid. The role of battery converter is not important in system operation as power is balanced by utility grid.

4.2.2. Autonomous mode

The battery plays very important role for both power balance and voltage stability. DC bus voltage is maintained stable by battery converter or boost converter. The main converter is controlled to provide stable and high quality AC bus voltage.

4.3.Modeling and control of converters

In the present work five types of converters are used for the proper coordination with utility grid which will be helpful for uninterrupted and high quality power to AC and DC loads under variable solar radiation and wind speed when grid operates in grid tied mode. The control algorithms are described in the following section.

4.3.1. Modeling and control of boost converter

The main objective of the boost converter is to track the maximum power point of the PV array by regulating the solar panel terminal voltage using the power voltage characteristic curve.

For the boost converter the input output equations can be written as

$$V_{pv} - V_T = L_1 \frac{di_1}{dt} + R_1 i_1 \quad (4.1)$$

$$I_{pv} - i_1 = C_{pv} \frac{dV_{pv}}{dt} \quad (4.2)$$

$$V_T = V_d(1 - d_1) \quad (4.3)$$

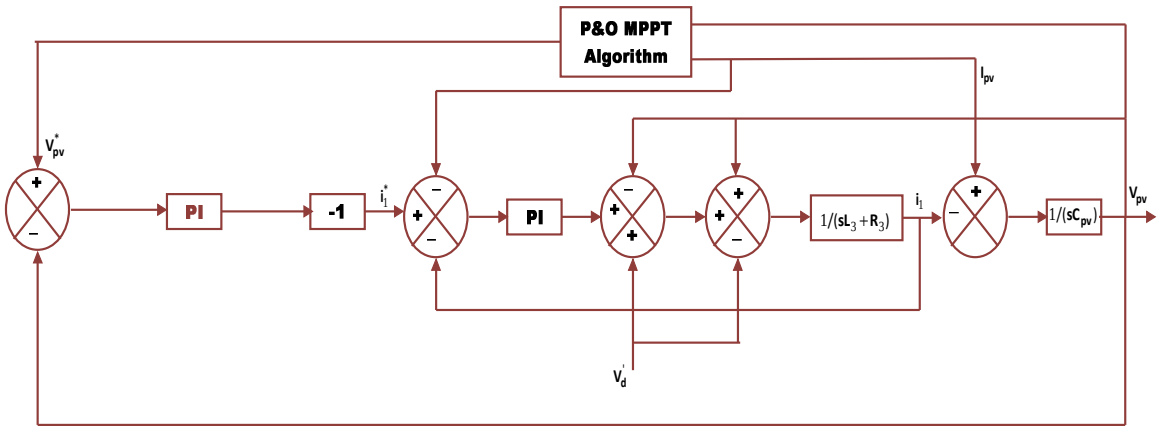

Fig 4.3. Control block diagram of boost converter

With the implementation of P&O algorithm a reference value i.e. V_{pv}^* is calculated which mainly depends upon solar irradiation and temperature of PV array [32]. Here for the boost converter dual loop control is proposed [33]. Here the control objective is to provide a high quality DC voltage with good dynamic response. The outer voltage loop helps in tracking of reference voltage with zero steady state error and inner current loop help in improvisation of dynamic response.

4.3.2. Modeling and control of main converter

The role of the main converter is to exchange power between AC and DC bus. The key purpose of main converter is to maintain a stable DC-link voltage in grid tied mode. When the converter operates in grid tied mode, it has to supply a given active and reactive power. Here PQ control scheme is used for the control of main converter. The PQ control is achieved using a current controlled voltage source. Two PI controllers are used for real and reactive power control. When resource conditions or load capacities change, the DC bus voltage is setteled to constant through PI regulation. The PI controller is set as the instantaneous active current i_{dm} reference and the instantaneous reactive current i_{qm} reference is determined by reactive power compensation command.

The model of the converter can be represented in ABC coordinate as

$$L_2 \frac{d}{dt}\begin{pmatrix} i_A \\ i_B \\ i_C \end{pmatrix} + R_2 \begin{pmatrix} i_A \\ i_B \\ i_C \end{pmatrix} = \begin{pmatrix} v_{SA} \\ v_{SB} \\ v_{SC} \end{pmatrix} - \begin{pmatrix} v_{CA} \\ v_{CB} \\ v_{CC} \end{pmatrix} \tag{4.4}$$

The above equation can be written in the d-q coordinate as

$$L_2 \frac{d}{dt}\begin{pmatrix} i_{dm} \\ i_{qm} \end{pmatrix} = \begin{pmatrix} -R_2 & \omega L_2 \\ -\omega L_2 & -R_2 \end{pmatrix}\begin{pmatrix} i_{dm} \\ i_{qm} \end{pmatrix} + \begin{pmatrix} v_{sd} \\ v_{sq} \end{pmatrix} - \begin{pmatrix} v_{cd} \\ v_{cq} \end{pmatrix} \tag{4.5}$$

Where (i_A, i_B, i_C) and (v_{CA}, v_{CB}, v_{CC}) are three phase current and voltages of the main converter. Three phase voltage of AC bus voltage are represented by the notations as (v_{SA}, v_{SB}, v_{SC}). The variables (i_{dm}, i_{qm}), (v_{cd}, v_{cq}), (v_{sd}, v_{sq}) are d-q coordinates of three phase currents, voltages of main converter and voltage of AC bus respectively.

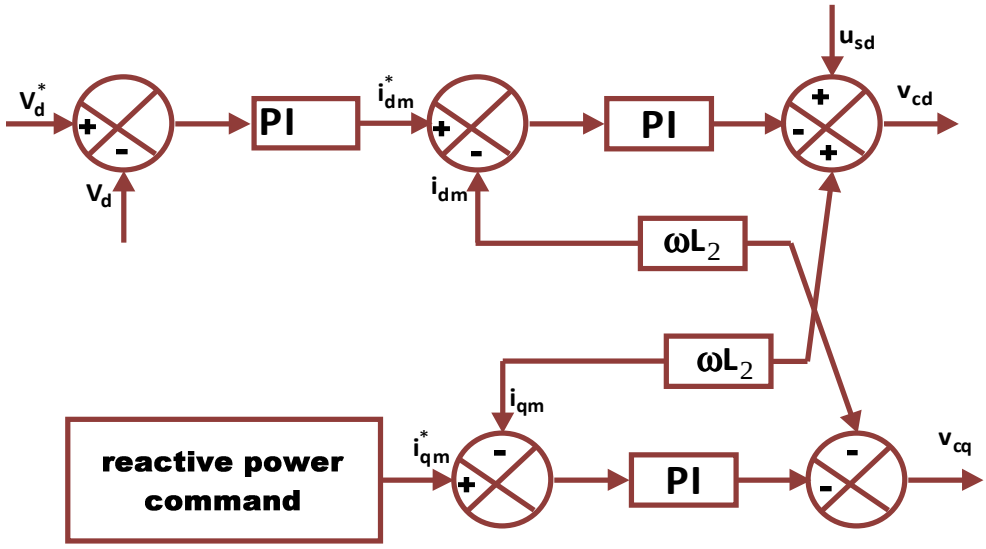

Fig 4.4. Control block diagram of main converter

In case of sudden DC load drop, there is power surplus at DC side and the main converter is controlled to transfer power from DC to AC side. The active power absorbed by the capacitor C_d leads to rising of DC-link voltage V_d. The negative error caused by the increase of V_d produces a higher active current reference i_{dm}^* through PI control. A higher positive reference i_{dm}^* will force active current reference i_{dm} to increase through the inner current control loop. Therefore the power surplus of the DC grid can be transferred to the AC side.

Also a sudden increase of DC load causes the power shortage and V_d drop at the DC grid. The main converter is controlled to supply power from the AC to DC side. The positive voltage error caused by V_d drop makes the magnitude of i_{dm}^* increase through the PI control. Since i_{dm} and i_{dm}^* are both negative, the magnitude of i_{dm} is increased through the inner current control loop. Hence power is transferred from AC grid to the DC side.

4.3.3. Modeling and control of DFIG

The section 3.2.1 explains the detailed modeling of DFIG. The state space equations are considered for induction machine modeling. The parameters and specifications of the DFIG are given in table 3.1. Flux linkages are used as the state variables in the model. Here two back to back converters are used in the rotor circuit. The main purpose of the machine-side

converter is to control the active and reactive power by controlling the d-q components of rotor current, while the grid-side converter controls the dc-link voltage and ensures the operation at unity power factor by making the reactive power drawn by the system from the utility grid to zero.

Two back to back converters are connected to the rotor circuit is shown in Fig 4.5. The firing pulses are given to the devices (IGBTs) using PWM techniques. Two converters are linked to each other by means of dc-link capacitor.

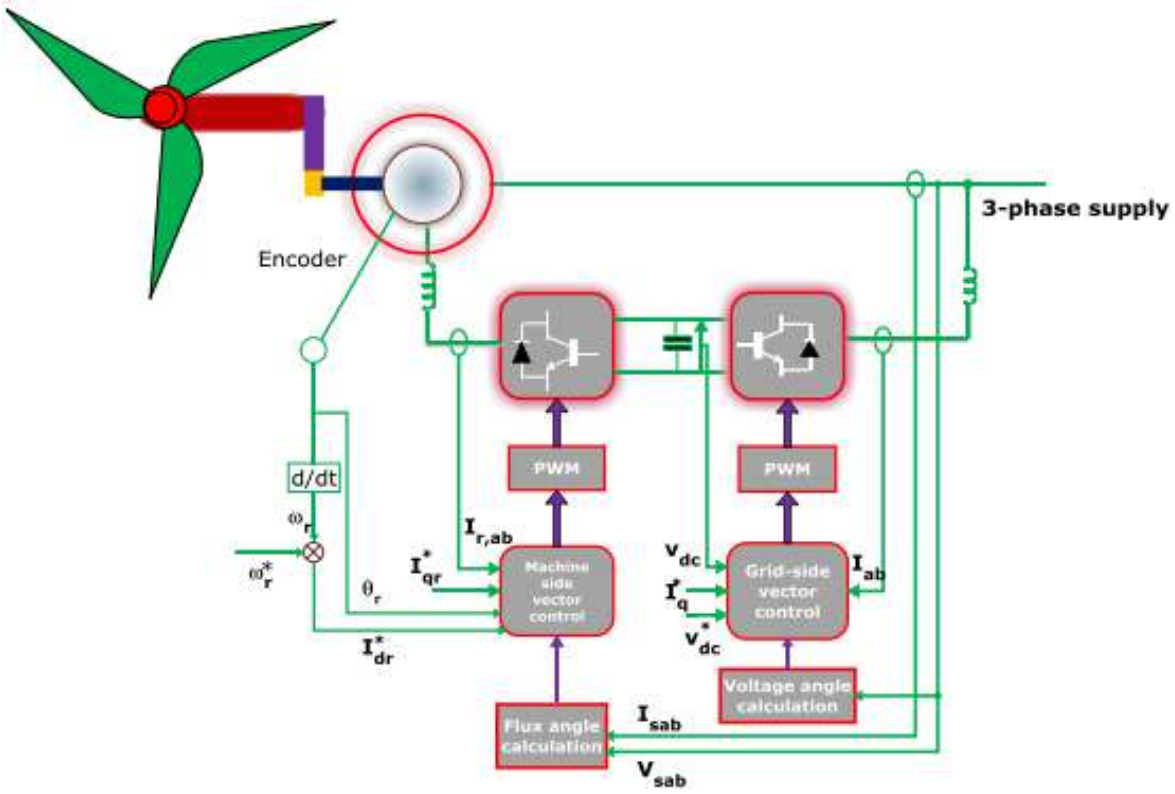

Fig. 4.5. Overall DFIG system

Basically converter 1 controls the grid parameters whereas the converter 2 serves for machine. The converters use six IGBTs (for three phase bridge type) as the controlled device. The PWM technique uses the controlled voltage v_a^*, v_b^*, v_c^*.The triangular career waves are being compared with sinusoidal reference waves to ensure pulses for the devices. The modulation indices are different for the both converters which are determined by the equation (4.6) & (4.7).

$$V_s = m_1 \frac{V_{dc}\sqrt{3}}{2\sqrt{2}} \tag{4.6}$$

$$V_r = \pm s\frac{V_s}{n} = m_2 \frac{V_{dc}}{2\sqrt{2}} \Longrightarrow s = \pm \frac{nm_2}{m_1\sqrt{3}} \tag{4.7}$$

4.3.3.1. Modeling and control of grid side converter

When the voltages in the grid changes due to different unbalance conditions, it makes an effect on the dc link voltage. The relation between stator voltage and the DC link voltage is represented by the equation (4.6) & (4.7).

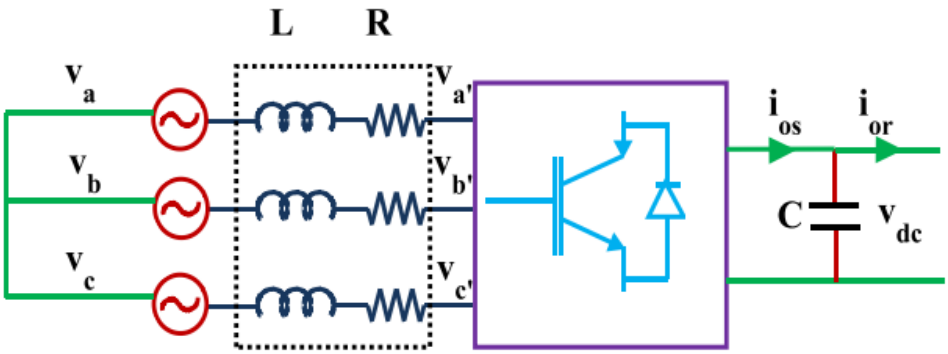

Fig 4.6. Schematic diagram of grid side converter

Since the machine is grid connected the grid voltage as well as the stator voltage is same, there exists a relation between the grid voltage and DC link voltage. The main objective of the grid side converter is to maintain DC link voltage constant for the necessary action. The voltage oriented vector control method is approached to solve this problem.

The detail mathematical modeling of grid side converter is given below. The control strategies are made following the mathematical modeling and it is shown in Fig. 4.7. The PWM converter is current regulated with the direct axis current is used to regulate the DC link voltage whereas the quadrature axis current component is used to regulate the reactive power. The reactive power demand is set to zero to ensure the unit power factor operation [35]. Fig. 4.6 shows the schematic diagram of the grid side converter.

The voltage balance across the line is given by Eq. (4.8), where R and L are the line resistance and reactance respectively. With the use of d-q theory the three phase quantities are transferred to the two phase quantities.

$$\begin{bmatrix} v_a \\ v_b \\ v_c \end{bmatrix} = R \begin{bmatrix} i_a \\ i_b \\ i_c \end{bmatrix} + L \frac{d}{dt} \begin{bmatrix} i_a \\ i_b \\ i_c \end{bmatrix} + \begin{bmatrix} v_{a'} \\ v_{b'} \\ v_{c'} \end{bmatrix} \tag{4.8}$$

For the grid side converter the mathematical modeling can be represented as

$$v_d = Ri_d + L\frac{di_d}{dt} - \omega_e L i_q + v_{dl} \tag{4.9}$$

$$v_q = Ri_q + L\frac{di_q}{dt} - \omega_e L i_d + v_{ql} \tag{4.10}$$

Where v_{d1} and v_{q1} are the two phase voltages found from $v_{a'}$, $v_{b'}$, $v_{c'}$ using d-q theory. Since the DC link voltage needs to be constant and the power factor of the overall system sets to be unity, the reference values are to be set consequently.

The d and q reference voltages are found from the Eq. (4.11) and (4.12).

$$v_d^* = v_d - i_d^* R + i_q^* \omega_e L - v_{d'} \tag{4.11}$$

$$v_q^* = v_q - i_q^* R + i_d^* \omega_e L - v_{q'} \tag{4.12}$$

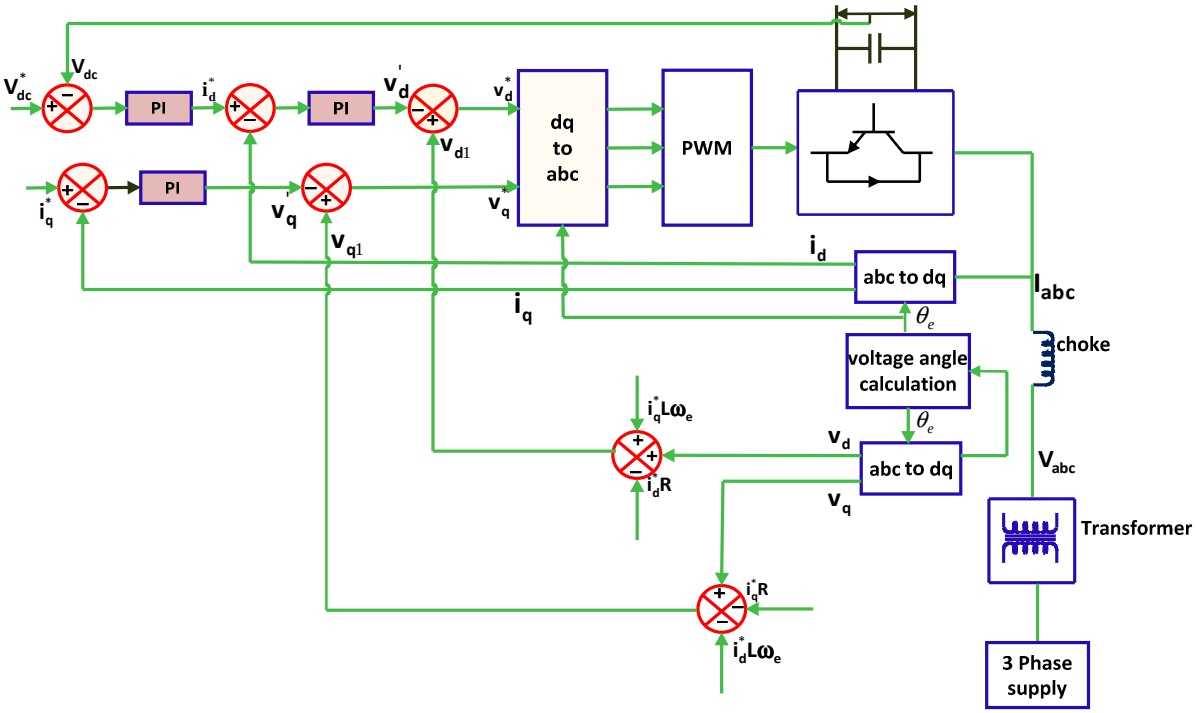

Fig 4.7. Control block diagram of grid side converter

The control scheme utilizes current control loops for i_d and i_q with the i_d demand being derived from the dc-link voltage error through a standard PI controller. The i_q demand determines the displacement factor on the grid side of the choke. The i_q demand is set to zero to guarantee unit power factor. There are two loops for the control design, i.e. inner current loop and outer voltage loop to provide necessary control action. Line resistance and reactance decide the plant for the current loop, whereas DC link capacitor is taken as the plant for the voltage loop. The plants for the current loop and the voltage loop are given in Eq. (4.13) and (4.14) respectively.

$$F(s) = \frac{i_d(s)}{v_{d'}(s)} = \frac{i_q(s)}{v_{q'}(s)} = \frac{1}{Ls+R} \tag{4.13}$$

$$G(s) = \frac{v_{dc}(s)}{i_d(s)} = \frac{3m_1}{2\sqrt{2}Cs} \tag{4.14}$$

The active and reactive power is controlled independently using the vector control strategy. Aligning the d-axis of the reference frame along the stator voltage position is found by Eq. (4.15), $v_q = 0$, since the amplitude of supply voltage is constant the active power and reactive power are controlled independently by means of i_d and i_q respectively following Eq. (4.16) and (4.17).

$$\tan\theta_e = \frac{v_q^s}{v_d^s} \tag{4.15}$$

$$P_s = \frac{3}{2}\left(v_d i_d + v_q i_q\right) \tag{4.16}$$

$$Q_s = \frac{3}{2}\left(v_d i_q + v_q i_d\right) \tag{4.17}$$

4.3.3.2. Modeling and control of machine side converter

The control strategy made for the machine side converter is shown in Fig.4.8. The main purpose of the machine side converter is to maintain the rotor speed constant irrespective of the wind speed and also the control strategy has been implemented to control the active power and reactive power flow of the machine using the rotor current components. The active power flow is controlled through i_{dr} and the reactive power flow is controlled through i_{qr}. To ensure unit power factor operation like grid side converter the reactive power demand is also set to zero here. The mathematical modeling of the machine side converter is given in the following equations [35].

Since the stator is connected to the utility grid and the influence of stator resistance is small, the stator magnetizing current i_m can be considered as constant. Under voltage orientation the relationship between the torque and the d-q axis voltages, currents and fluxes can be written as follows. Neglecting leakage inductances the stator flux Equations can be written as

$$\lambda_{ds} = 0 \tag{4.18}$$

$$\begin{aligned}\lambda_{qs} &= L_s i_{qs} + L_m i_{qr} \\ &= (L_{1s} + L_m) i_{qs} + L_m i_{qr} \\ &= L_{1s} i_{qs} + (i_{qs} + i_{qr}) L_m \approx L_m i_m\end{aligned} \tag{4.19}$$

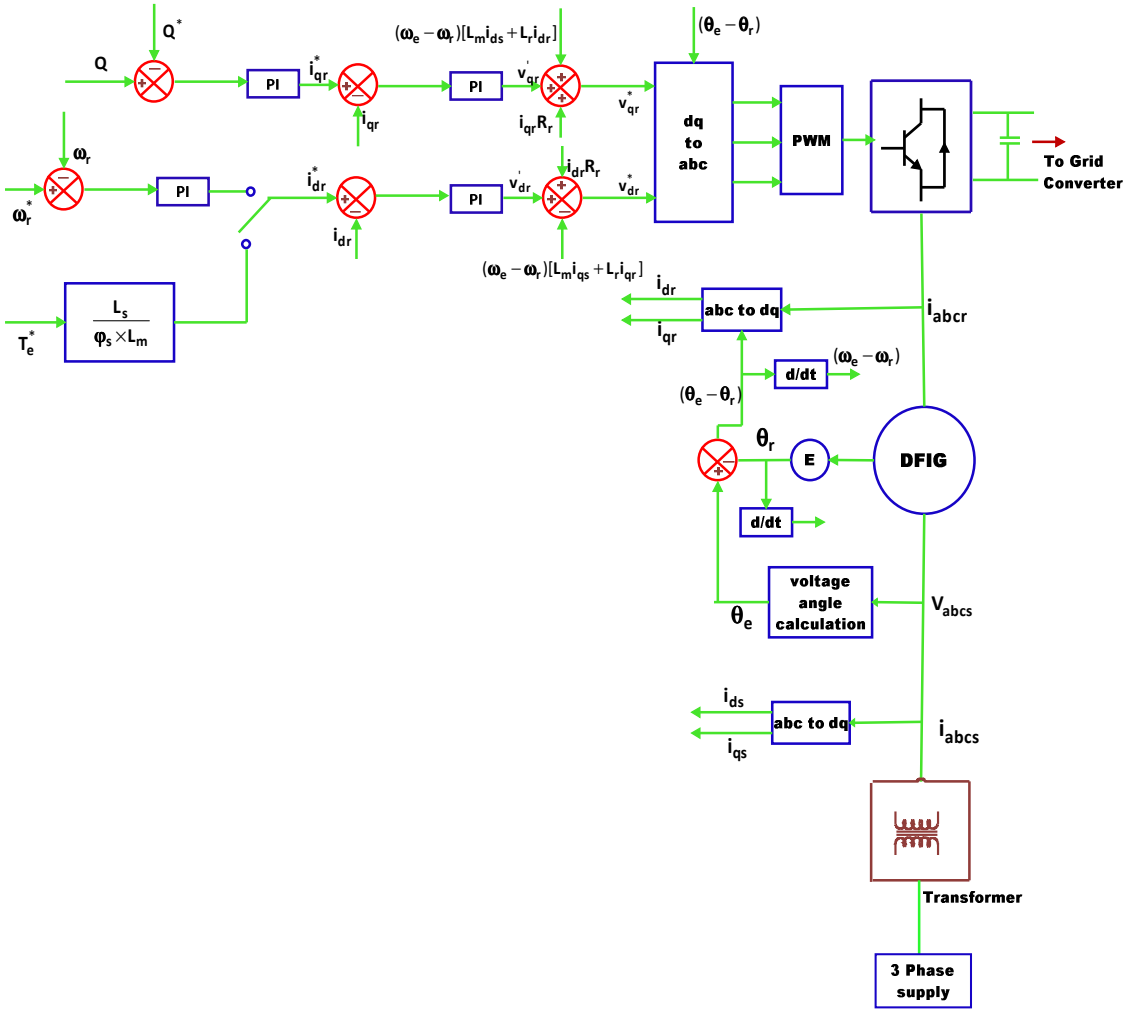

Fig 4.8. Control block diagram of machine side converter

The rotor voltage equations can be written from the equations (4.20) and (4.21).

$$v_{qr} = R_r i_{qr} + \frac{d}{dt}\left(\frac{L_m^2}{L_s} i_m + \sigma L_r i_{qr}\right) + (\omega_e - \omega_r)\sigma L_r i_{dr}$$

$$= R_r i_{qr} + \frac{d}{dt}\left(0 + \sigma L_r i_{qr}\right) + (\omega_e - \omega_r)\sigma L_r i_{dr} = R_r$$

$$= R_r i_{qr} + \sigma L_r \frac{d}{dt} i_{qr} + (\omega_e - \omega_r)\sigma L_r i_{dr} \quad (4.22)$$

$$v_{dr} = R_r i_{dr} + \sigma L_r \frac{di_{dr}}{dt} - (\omega_e - \omega_r)\left(\frac{L_m^2}{L_s} i_m + \sigma L_r i_{qr}\right) \quad (4.23)$$

The reference value V_{dr}^* and V_{qr}^* are given in Eq. (4.24) and (4.25) which are being found from Eq. (4.22) and (4.23).

$$v_{dr}^* = v'_{dr} + i_{dr} R_r - (\omega - \omega_r)\left[i_{qr} L_r + L_m i_{qs}\right] \quad (4.24)$$

$$v_{qr}^{*} = v'_{qr} + i_{qr}R_r - (\omega - \omega_r)[i_{dr}L_r + L_m i_{ds}] \quad (4.25)$$

Where v'_{dr} and v'_{qr} are found from the current errors processing through standard PI controllers. The reference current i_{dr}^{*} can be found either from the reference torque given by Eq. (4.27) or form the speed errors (for the purpose of speed control) through standard PI controllers. Similarly i_{qr}^{*} is found from the reactive power errors. The speed and reactive power is controlled using the current control loops.

The electromagnetic torque can be represented as

$$T_e = \frac{3}{2}\frac{P}{2}(\lambda_{ds}i_{qs} - \lambda_{qs}i_{ds})$$

$$= -\frac{3}{2}\frac{P}{2}(\lambda_{ds}i_{qs})$$

$$= -\frac{3}{2}\frac{P}{2}\lambda_{qs}\left(-\frac{L_m}{L_s}i_{dr}\right)$$

$$= \frac{3}{2}\frac{P}{2}\frac{L_m}{L_s}\lambda_{qs}i_{dr} \quad (4.26)$$

The value of i_{dr}^{*} is found using Eq. (4.26)

$$i_{dr}^{*} = \frac{T_e^{*} \times L_s}{\lambda_{qs} \times L_m} \quad (4.27)$$

Where $T_e^{*} = \frac{P_{mech} - P_{loss}}{\omega_r}$

$$P_{loss} = \text{mechanical losses} + \text{electrical losses}(P_{Cus} + P_{Cur})$$

Mechanical losses include friction and windage losses whereas electrical losses include stator copper loss and rotor copper losses. The maximum mechanical power can be extracted from the wind is proportional to the cube of the rotor speed. The plant for the current loop is decided by the line resistance and reactance, whereas dc link capacitor is taken as the plant for the voltage loop. The plants for the current loop and the voltage loop are given in Eq. (4.28) and (4.29) respectively.

$$F(S) = \frac{i_{dr}(S)}{v_{dr'}(S)} = \frac{i_{qr}(S)}{v_{qr'}(S)} = \frac{1}{\sigma Lr + R_r} \quad (4.28)$$

$$G(S) = -\frac{3PL_m}{4L_s\lambda_{qs}(Js+B)} = \frac{K}{(Js+B)} \quad (4.29)$$

4.3.4. Modeling and control of battery

The battery converter is a bidirectional DC/DC converter and the main purpose of the battery converter is to give assurance of stable DC link voltage.

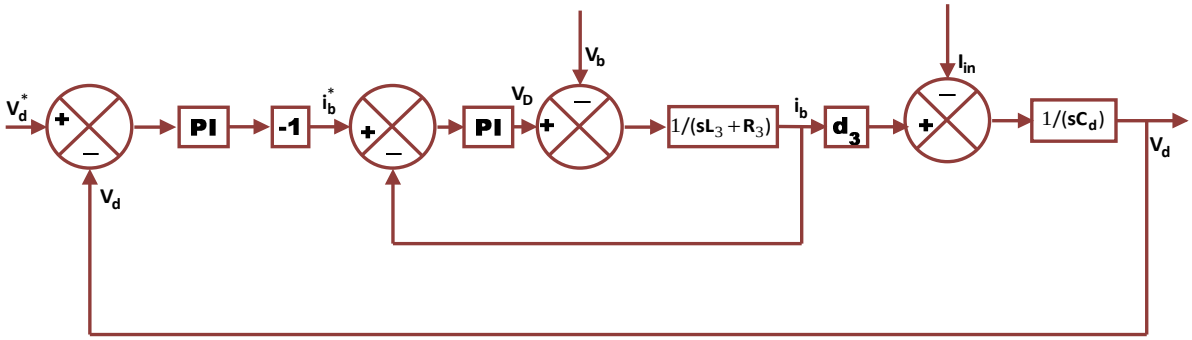

Fig 4.9. Control block diagram of battery

The boost converter injects current $i_1(1-d_1)$ to the DC link. The inverter and the DC loads draw current i_{ac} and i_{dc} from the DC link respectively.

The battery converter can be modeled as

$$V_D - V_b = L_3 \frac{di_b}{dt} + R_3 i_b \tag{4.30}$$

$$V_D = V_d \cdot d_3 \tag{4.31}$$

$$i_1(1-d_1) - i_{ac} - i_{dc} - i_b d_3 = C_d \frac{dV_d}{dt} \tag{4.32}$$

4.4. Summary

This chapter explains the configuration of the hybrid microgrid. Two modes of operation for the function of microgrid are also discussed. Also the modeling and control schemes for the used converters are analyzed in the above section.

CHAPTER 5

RESULT AND DISCUSSION

A hybrid microgrid whose parameters are given in table 4.1 is simulated using MATLAB/SIMULINK environment. The operation is carried out for the grid connected mode. Along with the hybrid microgrid, the performance of the doubly fed induction generator, photovoltaic system is analyzed. The solar irradiation, cell temperature and wind speed are also taken into consideration for the study of hybrid microgrid. The performance analysis is done using simulated results which are found using MATLAB.

5.1. Simulation of PV array

Figure (5.1)-(5.6) represents I-V, P-V, P-I characteristics with variation in temperature and solar irradiation. The nonlinear nature of PV cell is noticeable as shown in the figures, i.e., the output current and power of PV cell depend on the cell's terminal operating voltage and temperature, and solar irradiation as well.

Figures (5.1) and (5.2) verify that with increase of cell's working temperature, the current output of PV module increases, whereas the maximum power output reduces. Since the increase in the output current is much less than the decrease in the voltage, the total power decreases at high temperatures.

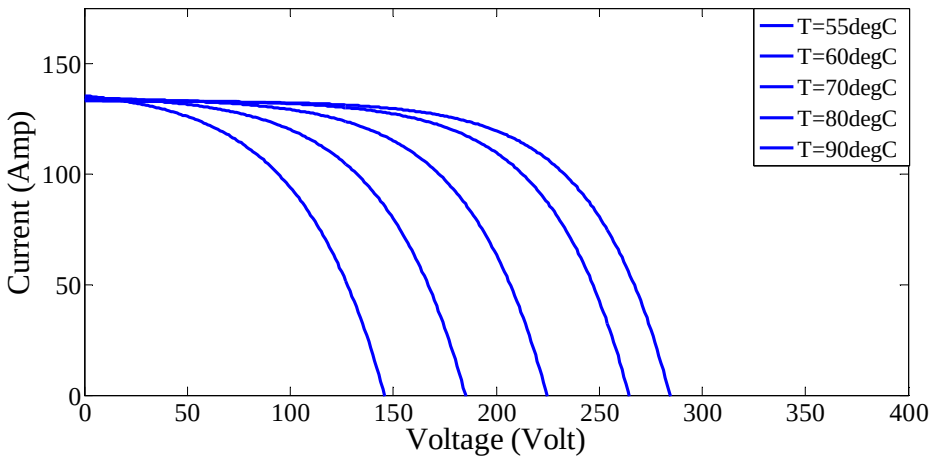

Fig 5.1. I-V output characteristics of PV array for different temperatures

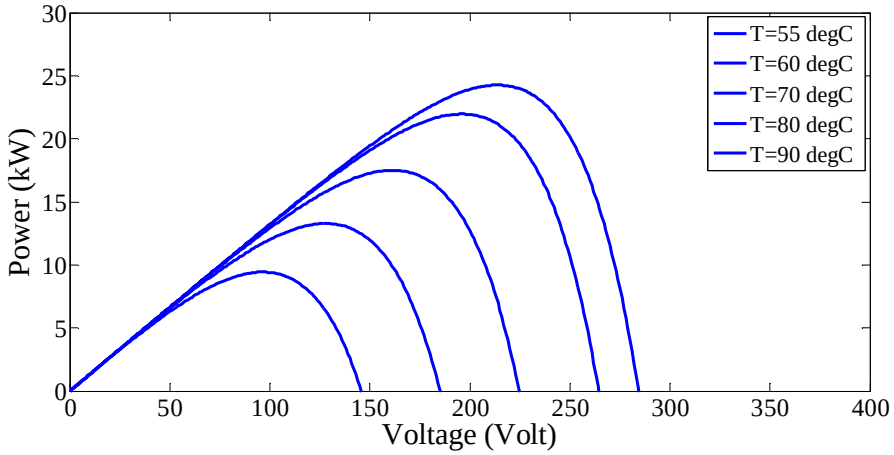

Fig 5.2. P-V output characteristics of PV array for different temperatures

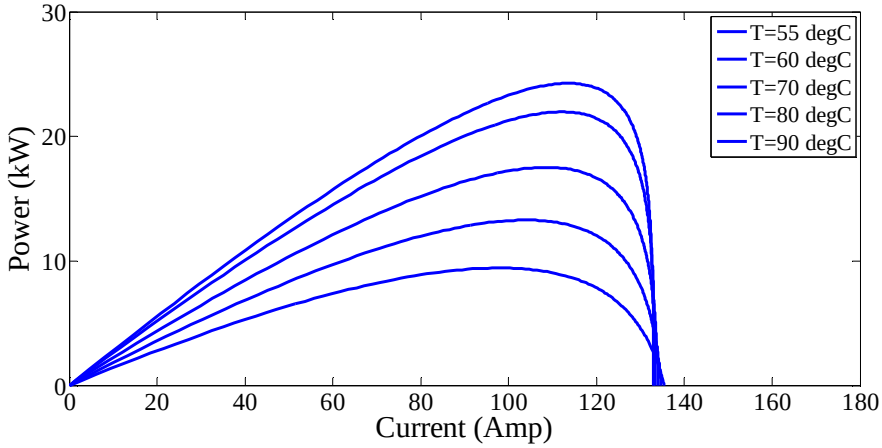

Fig 5.3. P-I output characteristics of PV array for different temperatures

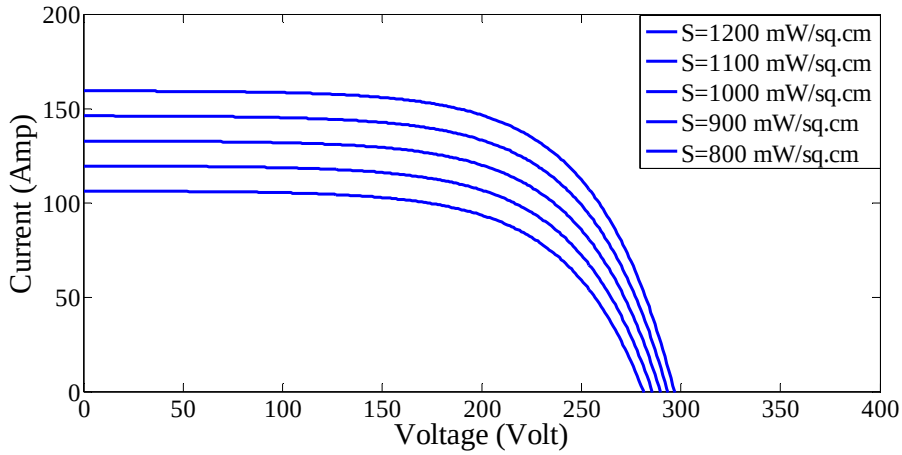

Fig 5.4. I-V output characteristics of PV array for different irradiance levels

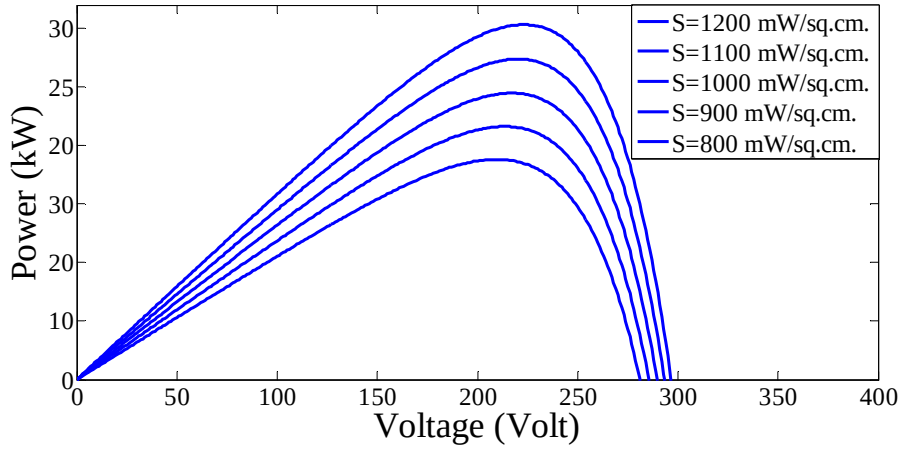

Fig 5.5. P-V characteristics of PV array for different irradiance levels

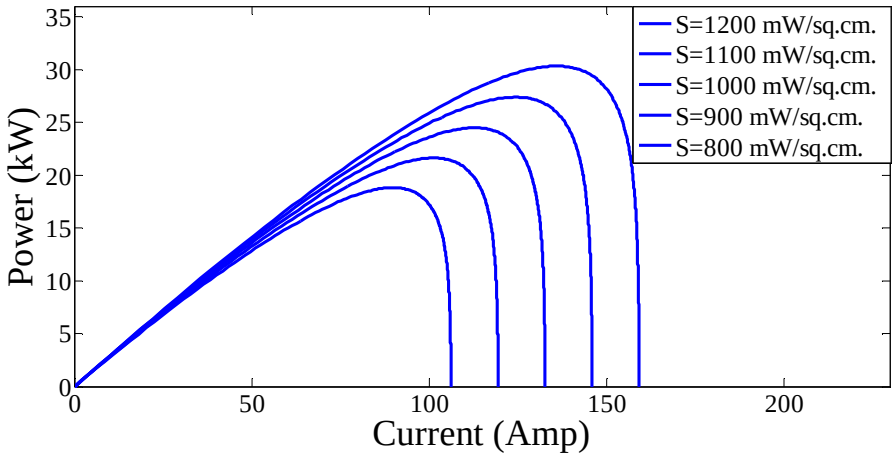

Fig 5.6. P-I characteristics of PV array for different irradiance levels

Figures (5.4) and (5.5) show that with increase of solar irradiation, the current output of PV module increases and also the maximum output power. The reason behind it is the open-circuit voltage is logarithmically dependent on the solar irradiance, however the short-circuit current is directly proportional to the radiant intensity.

5.2. Simulation of doubly fed induction generator

The response of wind speed, three phase stator voltage and three phase rotor voltage are shown in the figures (5.7) - (5.9). Here the value of wind speed varies between 1.0 to 1.05 pu which is necessary for the study of the performance of doubly fed induction generator. The phase to phase stator voltage is set to 300V whereas the rotor voltage value is 150V.

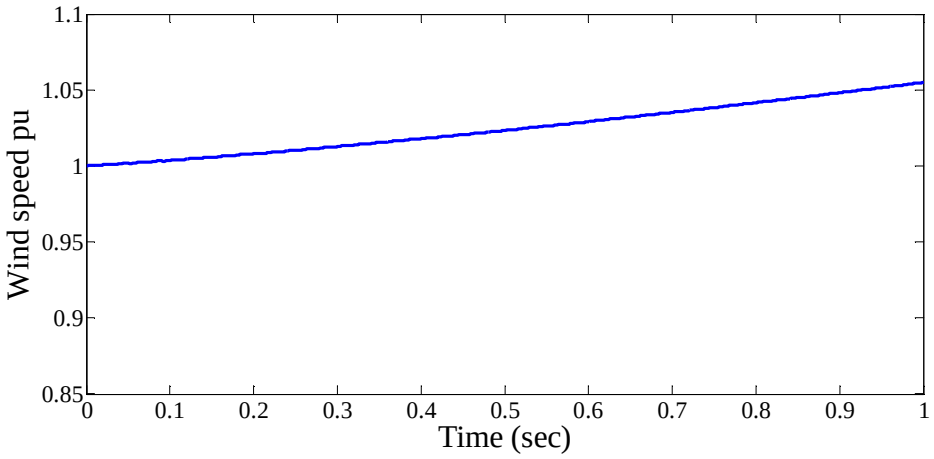

Fig 5.7. Response of wind speed

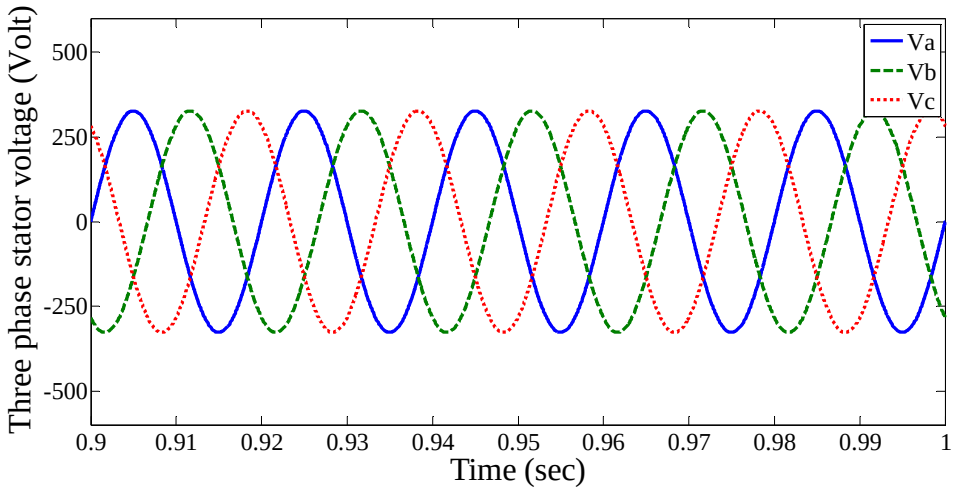

Fig 5.8. Three phase stator voltage of DFIG

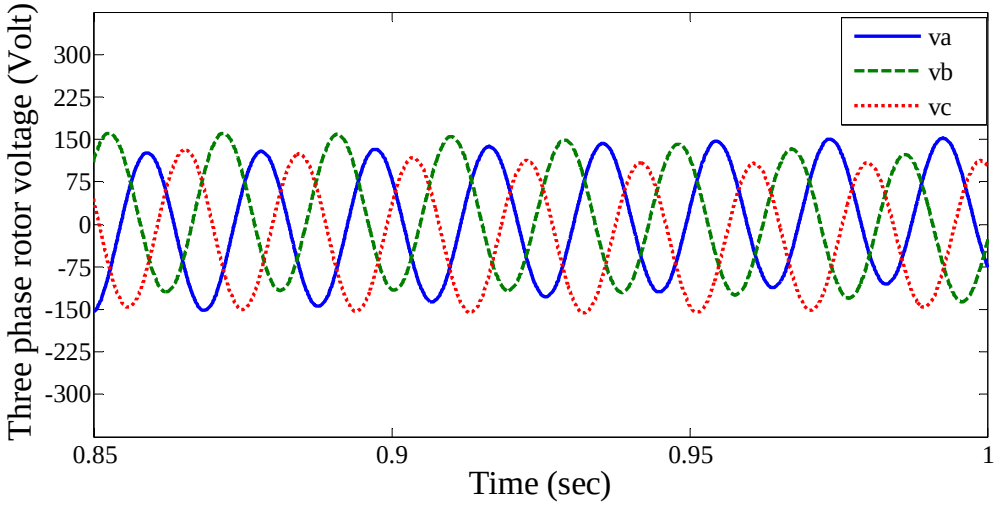

Fig 5.9. Three phase rotor voltage of DFIG

5.3. Simulation results of hybrid grid

The various characteristics of the hybrid microgrid are represented by the figures (5.10) – (5.25). Here the microgrid operates in the grid tied mode. In this mode, the main converter operates in the PQ mode and power is balanced by the utility grid. The battery is fully charged. AC bus voltage is maintained by the utility grid and DC bus voltage is maintained by the main converter.

Figure (5.10) shows the curve of solar irradiation level which value is set as 950 W/sq.m from 0.0s to 0.1s, increases linearly to 1300 W/sq.m from 0.1s to 0.2s, remains constant from 0.3s to 0.4s, decreases to 950 W/sq.m and keeps that value until 1s. Figures (5.11) – (5.13) signify output voltage, current and power with respect to the solar irradiation signal. The output power of PV panel varies 11.25 kW to 13 kW, which closely follows the solar irradiation when the ambient temperature is fixed.

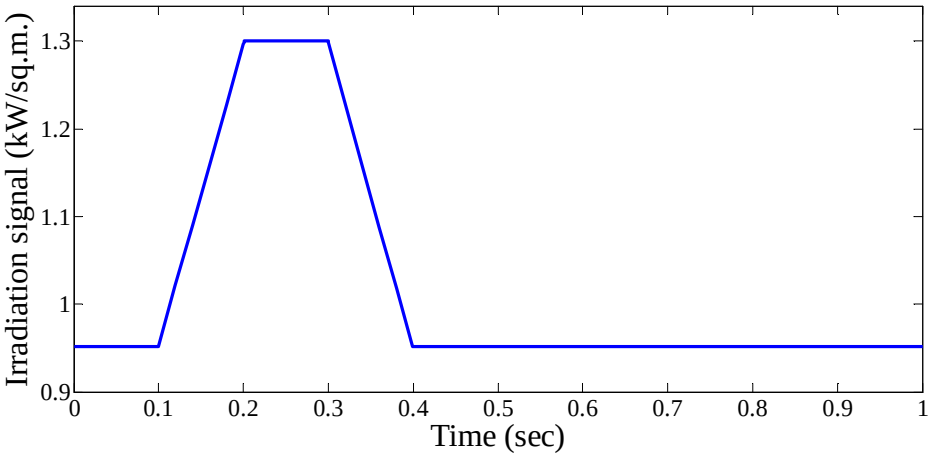

Fig 5.10. Irradiation signal of the PV array

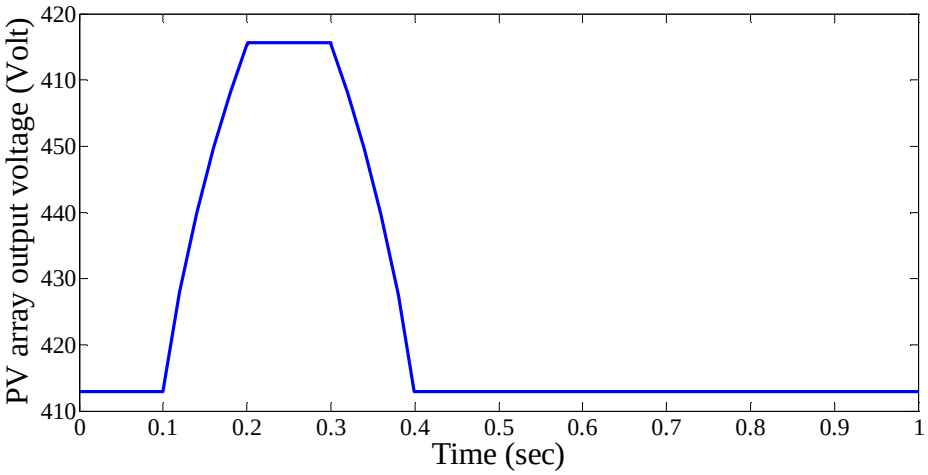

Fig 5.11. Output voltage of PV array

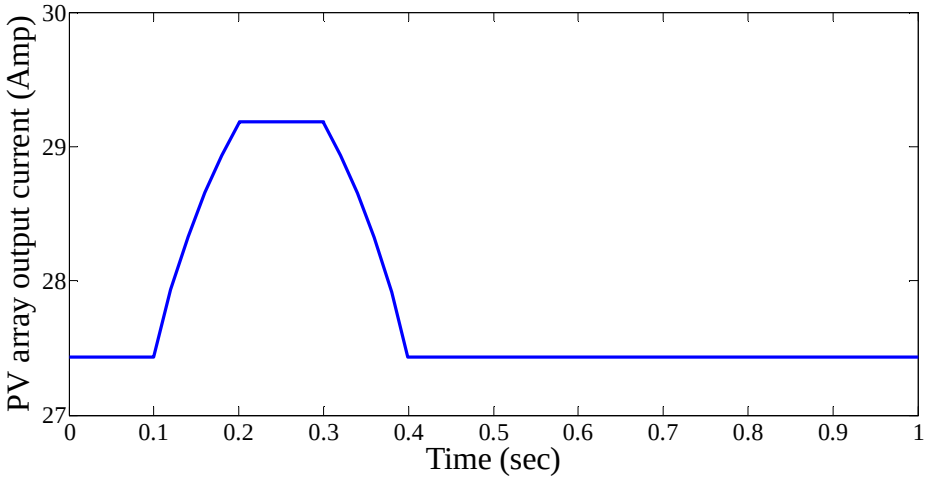

Fig 5.12. Output current of PV array

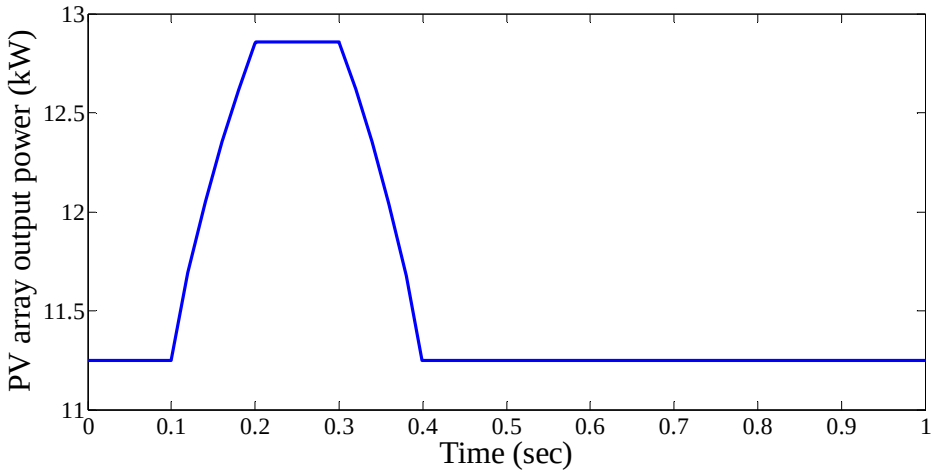

Fig 5.13. Output power of PV array

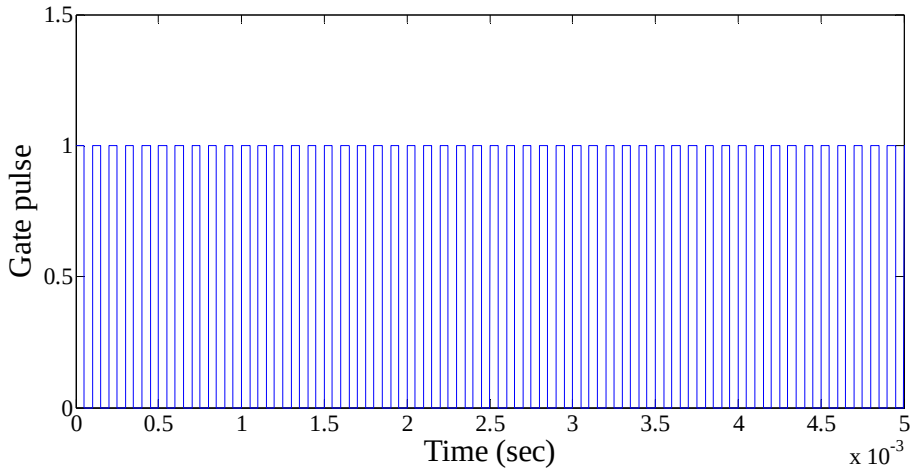

Fig 5.14. Generated PWM signal for the boost converter

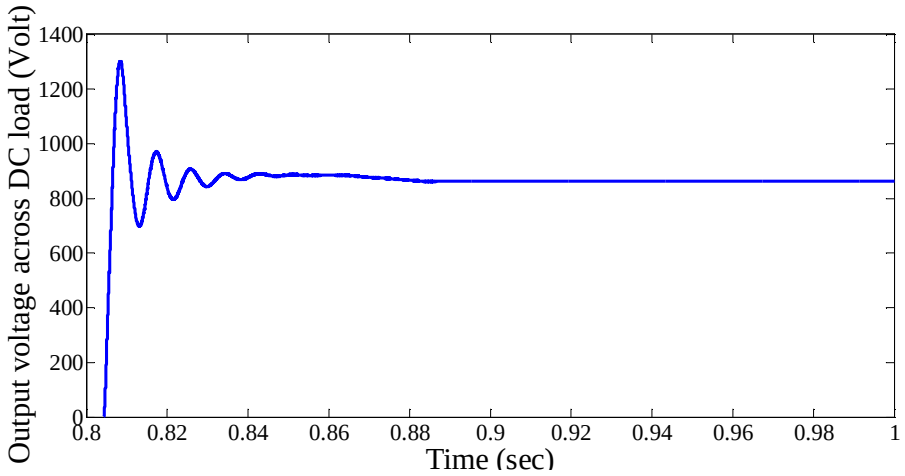

Fig 5.15. Output voltage across DC load

Figure (5.14) shows the gate pulse signal which is fed to the switch of boost converter. The output voltage across DC load is represented by figure (5.15) which is settled to around 820V.

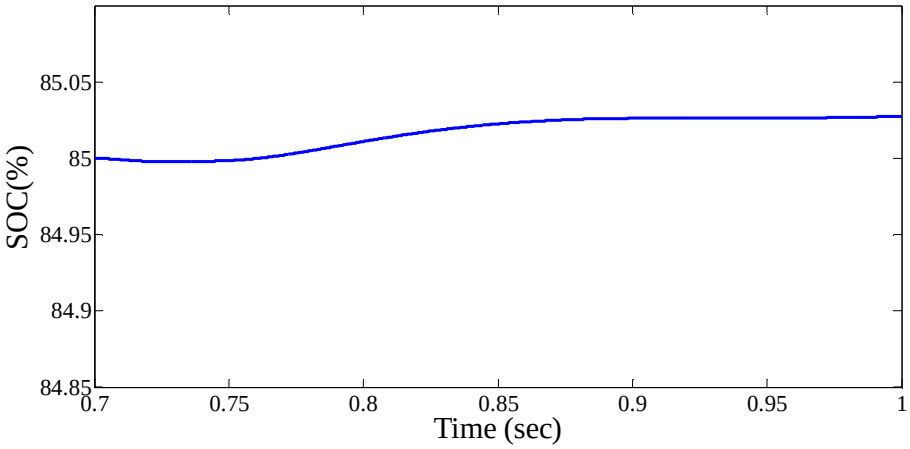

Fig 5.16. State of charge of battery

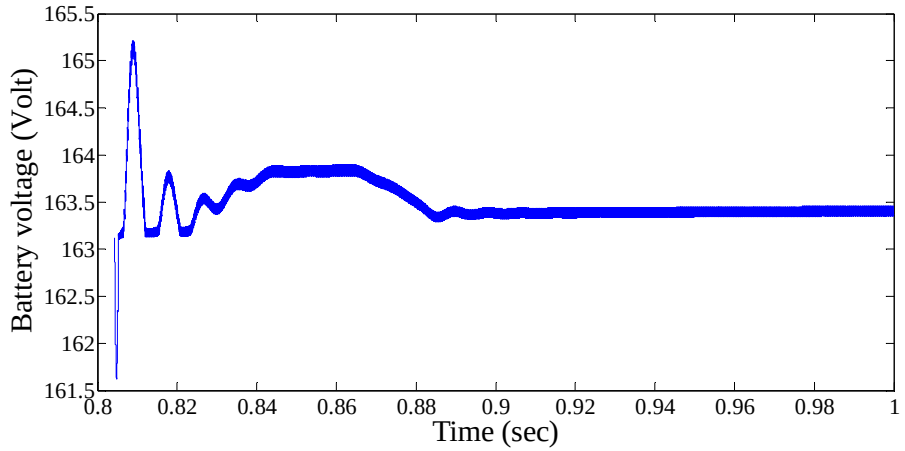

Fig 5.17. Voltage of battery

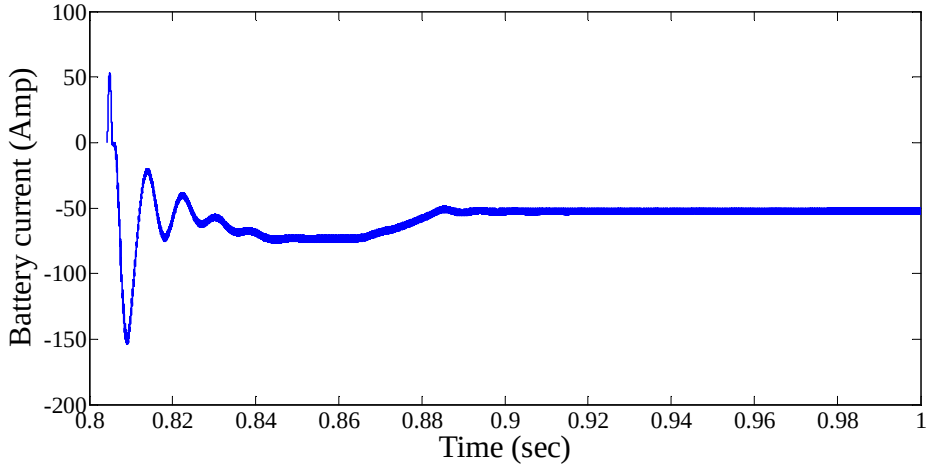

Fig 5.18. Current of battery

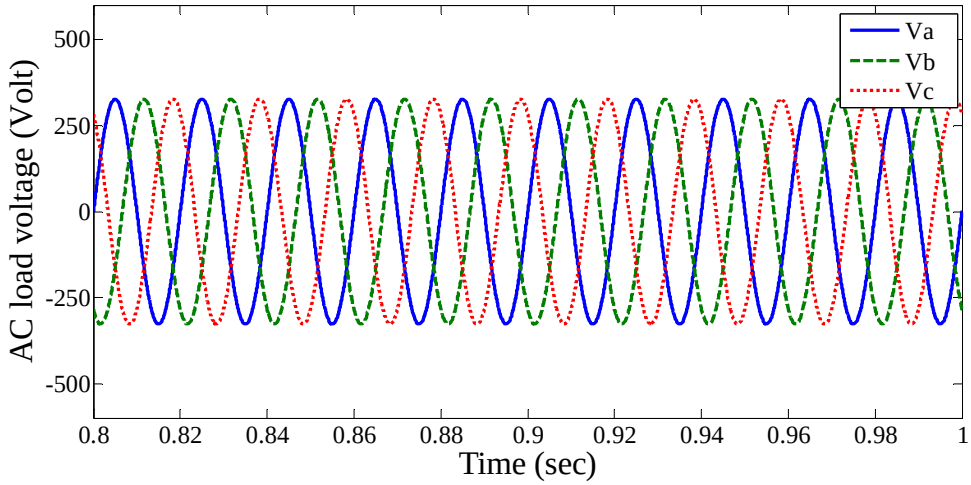

Fig 5.19. Output voltage across AC load

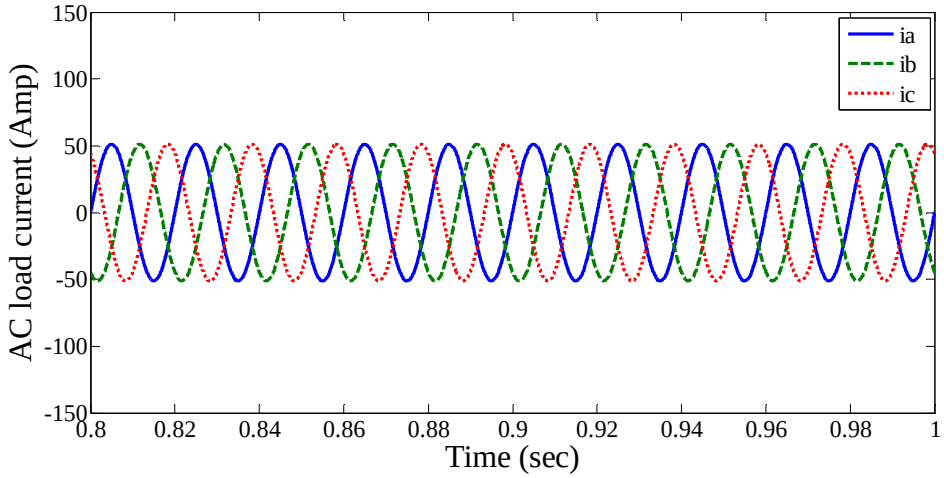

Fig 5.20. Output current across AC load

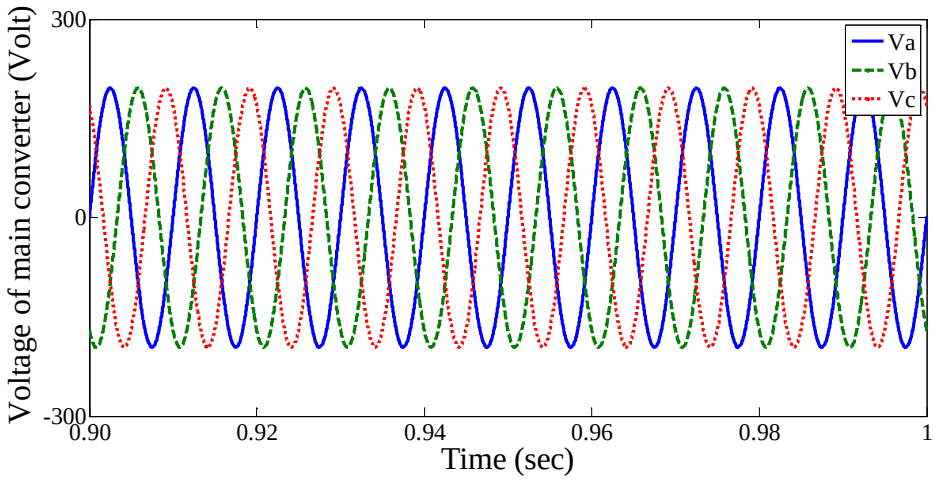

Fig 5.21. AC side voltage of the main converter

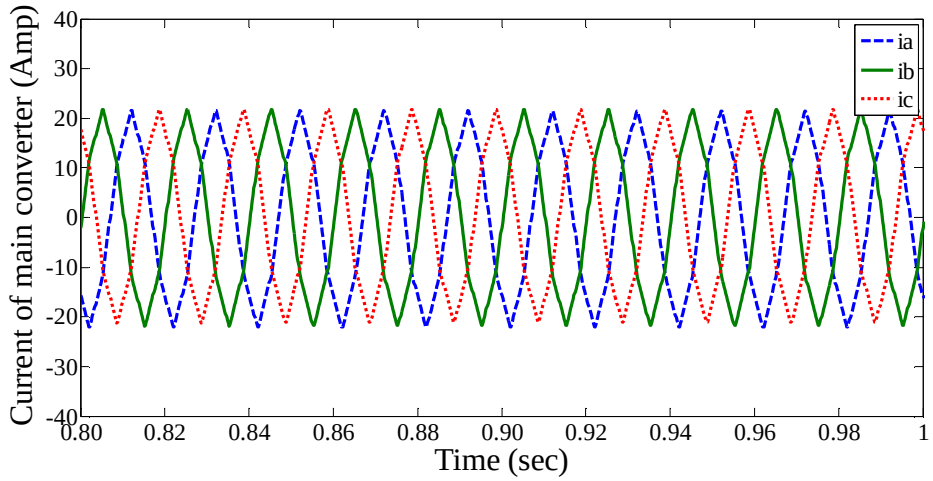

Fig 5.22. AC side current of the main converter

The battery characteristics are shown in the figures (5.16) - (5.18). The state of charge of battery is set at 85% whereas the battery current varies between -50 to 50A and the value of battery voltage is nearly 163.5. The output characteristics of AC load voltage and current are represented by the figures (5.19) and (5.20). Phase to phase voltage value of AC load is 300V and current value is 50A.Figure (5.21) and (5.22) shows the voltage and current responses at the AC side of the main converter when the solar radiation value varies between 950-1300 W/sq.m with a fixed DC load of 25 kW.

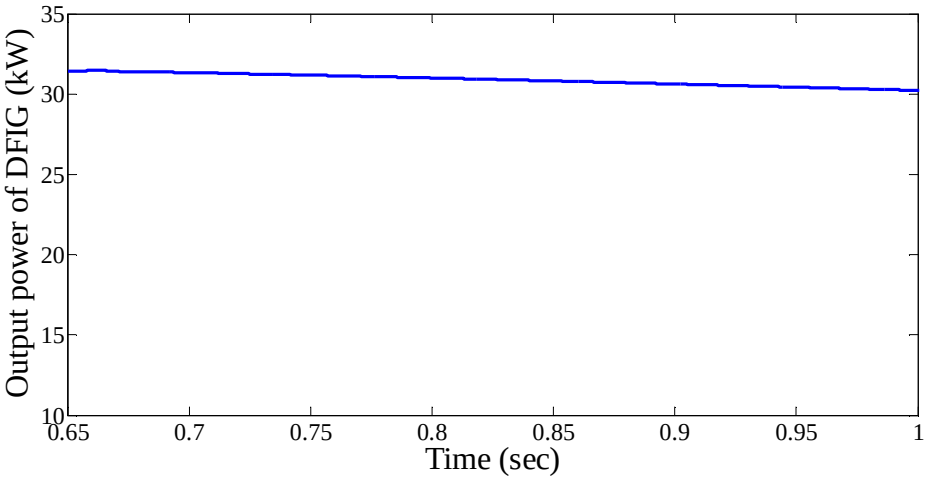

Fig 5.23. Output power of DFIG

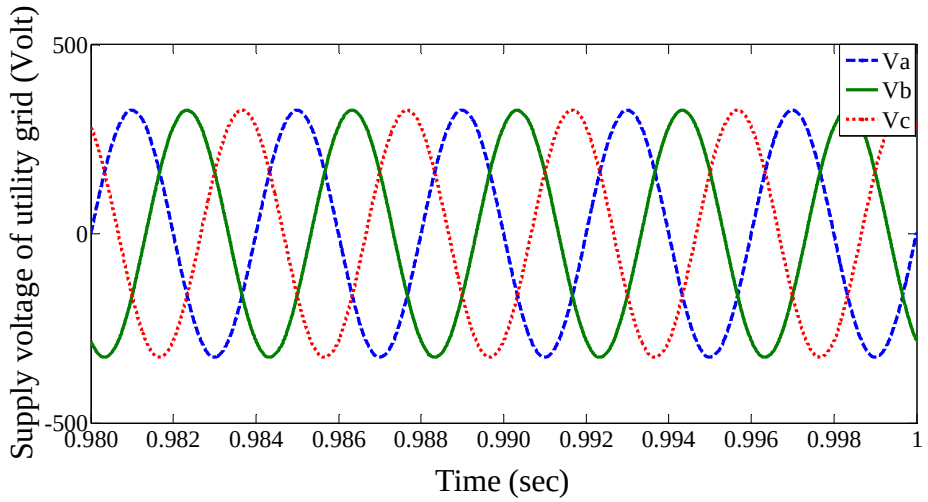

Fig 5.24. Three phase supply voltage of utility grid

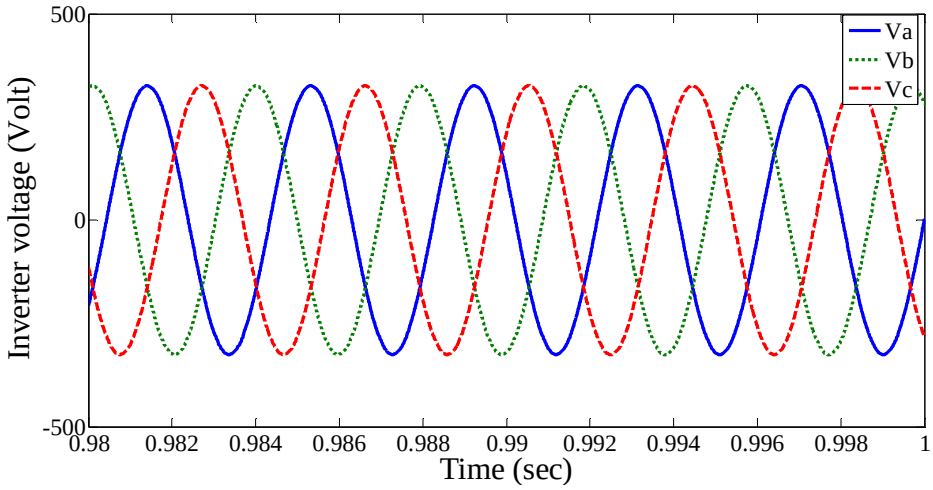

Fig 5.25. Three phase PWM inverter voltage

Figure (5.23) shows the response of the DFIG power output which becomes a stable value 32kW due to mechanical inertia. Figure (5.24) and (5.25) represents the three phase supply voltage to the utility grid and three phase PWM inverter output voltage respectively.

5.4. Summary

In this chapter simulation results are discussed briefly. Also various characteristics of PV array, doubly fed induction generator, battery and converters are studied in this chapter and the waveforms are traced.

CHAPTER 6

CONCLUSION AND SCOPE OF FUTURE WORK

6.1. Conclusion

The modeling of hybrid microgrid for power system configuration is done in MATLAB/SIMULINK environment. The present work mainly includes the grid tied mode of operation of hybrid grid. The models are developed for all the converters to maintain stable system under various loads and resource conditions and also the control mechanism are studied. MPPT algorithm is used to harness maximum power from DC sources and to coordinate the power exchange between DC and AC grid. Although the hybrid grid can diminish the processes of DC/AC and AC/DC conversions in an individual AC or DC grid, there are many practical problems for the implementation of the hybrid grid based on the current AC dominated infrastructure. The efficiency of the total system depends on the diminution of conversion losses and the increase for an extra DC link. The hybrid grid can provide a reliable, high quality and more efficient power to consumer. The hybrid grid may be feasible for small isolated industrial plants with both PV systems and wind turbine generator as the major power supply.

6.2. Scope of future work

a. The modeling and control can be done for the islanded mode of operation.
b. The control mechanism can be developed for a microgrid containing unbalanced and nonlinear loads.

References

[1] S. Bose, Y. Liu, K. Bahei-Eldin, J.de Bedout, and M. Adamiak, "Tie line Controls in Microgrid Applications," in *iREP Symposium Bulk Power System Dynamics and Control VII, Revitalizing Operational Reliability*, pp. 1-9, Aug. 2007.

[2] R. H. Lasseter, "MicroGrids," in *Proc. IEEE-PES'02*, pp. 305-308, 2002.

[3] Michael Angelo Pedrasa and Ted Spooner, "A Survey of Techniques Used to Control Microgrid Generation and Storage during Island Operation," in *AUPEC*, 2006.

[4] F. D. Kanellos, A. I. Tsouchnikas, and N. D. Hatziargyriou, "Microgrid Simulation during Grid-Connected and Islanded Mode of Operation," in *Int. Conf. Power Systems Transients (IPST'05)*, June. 2005.

[5] Y. W. Li, D. M. Vilathgamuwa, and P. C. Loh, Design, analysis, and real-time testing of a controller for multi bus microgrid system, *IEEE Trans. Power Electron.*, vol. 19, pp. 1195-1204, Sep. 2004.

[6] R. H. Lasseter and P. Paigi, "Microgrid: A conceptual solution," in *Proc. IEEE-PESC'04*, pp. 4285-4290, 2004.

[7] F. Katiraei and M. R. Iravani, "Power Management Strategies for a Microgrid with Multiple Distributed Generation Units," *IEEE trans. Power System*, vol. 21, no. 4, Nov. 2006.

[8] P. Piagi and R. H. Lasseter, "Autonomous control of microgrids," in *Proc. IEEE-PES'06*, 2006, *IEEE*, 2006.

[9] M. Barnes, J. Kondoh, H. Asano, and J. Oyarzabal, "Real-World MicroGrids- an Overview," in *IEEE Int. Conf. Systems of Systems Engineering*, pp.1-8, 2007.

[10] Chi Jin, Poh Chiang Loh, Peng Wang, Yang Mi, and Frede Blaabjerg, "Autonomous Operation of Hybrid AC-DC Microgrids," in *IEEE Int. Conf. Sustainable Energy Technologies*, pp. 1-7, 2010.

[11] Y. Zoka, H. Sasaki, N.Yomo, K. Kawahara, C. C. Liu, "An Interaction Problem of Distributed Generators Installed in a MicroGrid," in *Proc. IEEE Elect. Utility Deregulation, Restructuring and Power Technologies*, pp. 795-799, Apr. 2004.

[12] H. Nikkhajoei, R. H. Lasseter, "Microgrid Protection," in *IEEE Power Engineering Society General Meeting*, pp. 1-6, 2007.

[13] Zhenhua Jiang, and Xunwei Yu, "Hybrid DC- and AC-Linked Microgrids: Towards Integration of Distributed Energy Resources," in *IEEE Energy2030 Conf., pp.1*-8, 2008.

[14] Bo Dong, Yongdong Li, ZhixueZheng, Lie Xu "Control Strategies of Microgrid with Hybrid DC and AC Buses," in *Power Electronics and Applications, EPE'11, 14th European Conf.*, pp. 1-8, 2011.

[15] Dong Bo, Yongdong Li , and Zedong Zheng, "Energy Management of Hybrid DC and AC Bus Linked Microgrid," in *IEEE Int. Symposium Power Electronics for Distributed Generation System*, pp. 713-716, 2010.

[16] Xiong Liu, Peng Wang, and Poh Chiang Loh, "A Hybrid AC/DC Microgrid and Its Coordination Control," *IEEE Trans. Smart Grid*, vol. 2, no. 2, pp. 278-286 June. 2011.

[17] Mesut E. Baran, and Nikhil R. Mahajan, "DC Distribution for Industrial Systems: Opportunities and Challenges," *IEEE Trans. Industry Applications*, vol. 39, no. 6, pp. 1596-1601, Nov/Dec. 2003.

[18] Y. Ito, Z. Yang, and H. Akagi, "DC Microgrid Based Distribution Power Generation System," in *Proc. IEEE Int. Power Electron. Motion Control Conf.*, vol. 3, pp. 1740-1745, Aug. 2004.

[19] A. Arulampalam, N. Mithulananthan, R.C. Bansal, and T.K. Saba, "Microgrid Control of PV -Wind-Diesel Hybrid System with Islanded and Grid Connected Operations," in *Proc. IEEE Int. Conf. Sustainable Energy Technologies*, pp. 1-5, 2010.

[20] Poh Chiang Loh, Ding Li, and FredeBlaabjerg, "Autonomous Control of Interlinking Converters in Hybrid AC-DC Microgrid with Energy Storages," in *IEEE Energy Conversion Congress and Exposition (ECCE)*, pp. 652-658, 2011.

[21] M. E. Ropp and S. Gonzalez, "Development of a MATLAB/Simulink model of a single phase grid connected photovoltaic system," *IEEE Trans. Energy Conv.*, vol. 24, no. 1, pp. 195-202, Mar 2009.

[22] Mei Shan Ngan, Chee Wei Tan, "A Study of Maximum Power Point Tracking Algorithms for Stand-alone Photovoltaic Systems," in *IEEE Applied Power electronics Colloquium (IAPEC)*, pp. 22-27, 2011.

[23] K. H. Hussein, I. Muta, T.Hoshino, and M. Osakada, "Maximum Photovoltaic Power Tracking: An Algorithm for rapidly changing atmospheric conditions," in *Proc. Inst. Elect. Engg. Gener. Transm. Distrib.*, vol. 142, pp. 59–64, Jan.1995.

[24] D. P. Hohm, M. E. Ropp, "Comparative Study of Maximum Power Point Tracking Algorithms Using an Experimental, Programmable, Maximum Power Point Tracking Test Bed", in *IEEE*,pp.1699-1702, 2000.

[25] Marcello Gradella Villalva, Jones Rafael Gazoli, and Ernesto Ruppert Filho, “Analysis and Simulation of the P&O MPPT Algorithm using a linearized PV Array model,” in *Industrial Electronics, IECON’09, 35th Annual Conf.*, pp. 189-195, 2009.

[26] Mohammad A. S. Masoum, Hooman Dehbonei, and Ewald F. Fuchs, “Theoretical and Experimental Analyses of Photovoltaic Systems with Voltage- and Current-Based Maximum Power-Point Tracking”, in *IEEE Trans. Energy Conversion*, vol. 17, no. 4, pp. 514-522, Dec. 2002.

[27] O. Tremblay, L. A. Dessaint, and A. I. Dekkiche, “A generic battery model for the dynamic simulation of hybrid electric vehicles,” in *Proc. IEEE Veh. Power propulsion Conf.*, pp. 284-289, 2007.

[28] S. N. Bhadra, D. Kastha, S. Banerjee, “Wind Electrical Systems,” Oxford University Press, New Delhi, 2009.

[29] B. K. Bose, “Modern Power Electronics and AC Drives,” Prentice-Hall, Inc., New Delhi, 2002.

[30] A. Girgis and S. Brahma, "Effect of Distributed Generation on Protective Device Coordination in Distribution System," in *Large Engineering Systems Conf. Power Engineering*, pp. 115-119, 2001.

[31] N. Kroutikova, C. A. Hernandez-Aramburo, and T. C. Green, “State-space model of grid connected inverters under current mode control,” *IET Elect. Power Appl.*, vol. 1, no. 3, pp. 329-338, 2007.

[32] D. Sera, R. Teodorescu, J. Hantschel, and M. Knoll, “Optimized maximum power point tracker for fast-changing environmental conditions,” *IEEE Trans. Ind. Electron.*, vol.55, no. 7, pp. 2629-2637, Jul. 2008.

[33] B. Bryant and M. K. Kazimierczuk, “Voltage loop of boost PWM DC-DC converters with peak current mode control,” *IEEE Trans. Circuits Syst. I, Reg. Papers*, vol. 53, no. 1, pp. 99-105, Jan. 2006.

[34] S. Arnalte, J. C. Burgos, and J. L. Rodriguez-amenedo, “Direct torque control of a doubly fed induction generator for variable speed wind turbines,” *Elect. Power Compon. Syst.*, vol. 30, no. 2, pp. 199-216, Feb. 2002.

[35] R. Pena, J. C. Clare, G. M. Asher, “Doubly fed induction generator using back to back PWM converters and its application to variable speed wind energy generation,” in *Proc. IEE Electr. Power Appl.*, vol. 143, no. 3, pp. 231-241, may 1996.